



Cite this: *J. Mater. Chem. B*, 2020, **8**, 6765

Received 9th March 2020,  
Accepted 30th March 2020

DOI: 10.1039/d0tb00649a

[rsc.li/materials-b](http://rsc.li/materials-b)

## Overcoming the biological barriers in the tumor microenvironment for improving drug delivery and efficacy

Yang Zhou,<sup>a</sup> Xianchun Chen,<sup>b</sup> Jun Cao<sup>cd\*</sup> and Huile Gao<sup>id\*</sup>

The delivery of drugs to tumors by nanoparticles is a rapidly growing field. However, the complex tumor microenvironment (TME) barriers greatly hinder drug delivery to tumors. In this study, we first summarized the barriers in TME, including anomalous vasculature, rigid extracellular matrix, hypoxia, acidic pH, irregular enzyme level, altered metabolism pathway and immunosuppressive conditions. To overcome these barriers, many strategies have been developed, such as modulating TME, active targeting by ligand modification and biomimetic strategies, and TME-responsive drug delivery strategies to improve nanoparticle penetration, cellular uptake and drug release. Although extensive progress has been achieved, there are still many challenges, which are discussed in the last section. Overall, we carefully discuss the landscape of TME, development for improving drug delivery, and challenges that need to be further addressed.

<sup>a</sup> Key Laboratory of Drug-Targeting and Drug Delivery System of the Education Ministry, Sichuan Engineering Laboratory for Plant-Sourced Drug and Sichuan Research Center for Drug Precision Industrial Technology, West China School of Pharmacy, Sichuan University, Chengdu, 610064, China. E-mail: gao huile@scu.edu.cn, gao huile@163.com

<sup>b</sup> College of Material Science and Engineering, Sichuan University, Chengdu, 610064, China

<sup>c</sup> National Engineering Research Center for Biomaterials, Sichuan University, Chengdu, 610064, China. E-mail: caojun@scu.edu.cn

<sup>d</sup> Department of Biomedical Engineering, The University of Texas at Austin, Austin, TX, USA. E-mail: caojun@utexas.edu

<sup>e</sup> Division of Molecular Pharmaceutics and Drug Delivery, College of Pharmacy, The University of Texas at Austin, Austin, TX, USA

### 1. Introduction

Tumors are the second leading cause of death worldwide, threatening the lives of tens of millions of people.<sup>1,2</sup> Although substantial drugs have been developed, their delivery is far from satisfactory. Regardless of oral administration or intravenous injection, drug delivery to tumors primarily depends on the chemical properties of the drugs, such as molecular weight, hydrophobicity and chemical units, which is plagued by enzymolysis and rapid clearance from circulation. To circumvent these problems, nanoparticles (herein referring to all particles



Yang Zhou

Yang Zhou received her BS Degree in pharmacy from West China School of Pharmacy in Sichuan University in 2018. Currently, she is pursuing her PhD degree under the supervision of Professor Huile Gao. Her current research mainly focuses on the development and biomedical applications of functional nanomaterials for cancer therapy.



Xianchun Chen

Xianchun Chen is an Associated Professor at Sichuan University. She obtained her PhD in Materials Science from Sichuan University in 2010 and then joined Prof. Guangfu Yin's group in the College of Material Science and Engineering, Sichuan University as a Lecturer. From 2014 to 2017, she was engaged in the management of scientific research projects in the Ministry of Science and Technology of China. Her research interests focus on the material design of nanocarriers for drug delivery.

in the nanometer scale, NPs), including organic (*e.g.*, lipid-based, polymer-based and cell-derived NPs) and inorganic NPs (*e.g.*, gold, silver, iron oxide and silica), have been developed to deliver drugs for cancer therapy, also termed “nanomedicine”.<sup>3–5</sup> The basis for the design of current NPs is the enhanced permeability and retention (EPR) effect, where the hyperpermeable tumor vasculature allows the extravasation and passive diffusion of large particles coupled with impaired lymphatic drainage, reducing the elimination of NPs; thus, NPs are further retained and accumulate within tumors.<sup>6,7</sup> Besides, NPs can enhance drug stability and extend the circulation half-life.

Unfortunately, the clinical translation of nanomedicine still faces undesirable anti-tumor performances<sup>8</sup> despite the achievement of some progress in lowering off-target side effects.<sup>9</sup> As reported in a previous review, the median delivery efficiency of NPs into tumors is estimated to be merely 0.7% of an injected dose, completely diverging from the optimistic anticipation of nanomedicine.<sup>10</sup> Accordingly, the golden standard in drug delivery, *i.e.*, the EPR effect is somewhat oversimplified or exaggerated. In fact, for NPs, there is a long and bumpy journey to reach tumor cells. Besides abnormal vascular networks, other components in the tumor microenvironment (TME) play an essential role in deciding the *in vivo* fate of NPs. TME refers to all the physiological and biochemical compositions around tumor cells, which comprise various types of growth-supporting cells, fortified by a dense extracellular matrix (ECM) and irregular vascular networks.<sup>11</sup> These cells consist of endothelial cells, pericytes, cancer-associated fibroblasts (CAFs) and immune-infiltrating cells, while ECM consists of collagens, fibronectin, integrins, elastin, and microfibrillar proteins. These compositions interweave with each other and provide a niche for tumor development, progression and metastasis.<sup>12</sup> For NP-mediated anti-tumor therapy, some of the characteristics of TME, such as a high interstitial fluid pressure (IFP) and solid pressure, can impede drug delivery within the deep regions of tumors, while others, such as hypoxia and acidity, attenuate the antitumor effect and even cause drug resistance and metastasis.<sup>13</sup> For example, photodynamic therapy (PDT) and radiotherapy, which

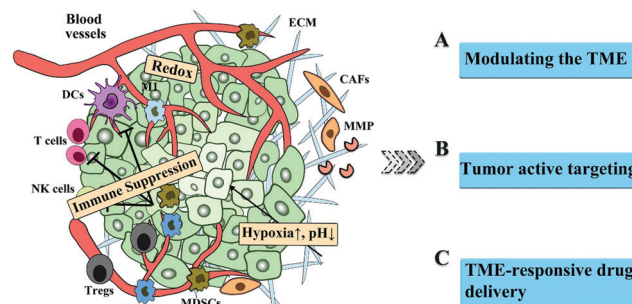


Fig. 1 Schematic illustration of the barriers in the TME and the corresponding strategies for improved drug delivery.

are dependent on oxygen, are greatly restricted by hypoxia in tumor tissues. Thus, it is important to elucidate the biological barriers in TME and modulate these TME targets, which can help NPs overcome the barriers to enhance their delivery efficiency and therapeutic effectiveness.

In this perspective, we summarize the barriers in the TME, presenting the landscape of the TME. Subsequently, we review the strategies to overcome the barriers in the TME, including modulating the TME, active tumor targeting, and TME-sensitive drug delivery, as shown in Fig. 1. Finally, the challenges to overcome the TME barriers are discussed.

## 2. Barriers in the TME

Increasing evidence has indicated drug delivery using nanocarriers is, to a large extent, hindered by the tumor heterogeneity, including anomalous vasculature, rigid ECM, hypoxia, acidic pH, overproduced glutathione (GSH) and reactive oxygen species (ROS), and immune suppression, which are derived from cancer cells, and the crosstalk between them and the TME.<sup>14,15</sup> Thus, the brief introduction of the dynamic tumor landscape will offer researchers better access to the developing direction of drug delivery in the future.



Jun Cao

*Jun Cao is an Associate Professor and a member of the National Engineering Research Center for Biomaterials and the Engineering Research Center in Biomaterials at Sichuan University. She received her PhD degree from the College of Polymer Science and Engineering at Sichuan University in 2013. Her current research interests focus on the design and synthesis of various smart polymers as drug delivery carriers for tumor diagnosis and therapy.*



Huile Gao

*Huile Gao is a Professor at Sichuan University. He obtained his PhD in Pharmaceutics from Fudan University in 2013 and then joined West China School of Pharmacy, Sichuan University as a lecturer. In 2017, Gao was promoted as a Professor. His research focuses on the rational design of drug delivery systems for central nervous system diseases and tumors.*

## 2.1 TME composition

Strictly, a favourable vascular network is an essential prerequisite for the effective delivery of nanomedicine. However, this is not the case with tumors. The overgrowth of neoplastic cells demands dramatically more nutrients relative to normal cells. Consequently, they and the surrounding stromal cells secret angiogenic growth factors, such as vascular endothelial growth factor (VEGF), basic fibroblast growth factor and tumor necrosis factor (TNF), leading to substantial vessel growth.<sup>16</sup> Notably, these newly-formed vessels are tortuous and leaky since aggressive angiogenesis is accompanied by a lack of paracellular junctions between endothelial cells and incomplete pericyte coverage.<sup>14,17,18</sup> As discussed earlier, the “leaky” gaps and blockage of lymphatic return provide evidence for the EPR effect.<sup>19</sup> However, this feature of the tumor vasculature is a double-edged sword. Excessive plasma and fluid can extravasate from leaky vessels to the interstitium, resulting in elevated IFP and viscosity,<sup>15</sup> while poor lymphatic drainage aggravates the IFP, and thus causes blood reversal and further retards blood flow. Accordingly, abnormally high IFP becomes a daunting bottleneck limiting the penetration and accumulation of NPs. Similarly, it also provides the possibility of tumor metastasis or drug resistance. Additionally, the tortuous nature of vessels can result in geometric obstruction against blood flow. Thus, the Janus-faced nature of aberrant vascular networks should be considered carefully for drug delivery mediated by passive targeting.

The tumor stroma is another roadblock, which comprises ECM, CAFs, mesenchymal stromal cells, osteoblasts, and chondrocytes.<sup>20</sup> Unlike quiescent fibroblasts in normal tissues, CAFs are activated to enhance the proliferation, migration, and secretion of multiple cytokines, such as VEGF, TNF, interleukin-6 (IL-6), platelet-derived growth factor (PDGF) and transforming growth factor-beta (TGF- $\beta$ ), which support tumor growth and render tumor resistance towards traditional chemotherapeutics.<sup>21,22</sup> More importantly, CAFs generate large amounts of ECM components, such as collagen and proteoglycans, which together offer a breeding ground for tumors. They also release vast enzymes, such as matrix metalloproteases (MMPs), disintegrins and plasmin, to degrade and remodel the ECM. Besides the intrinsic mesh-like physical resistance, the stiff stroma can elevate solid stress, increase IFP and isolate tumors from blood vessels, thus compromising the interstitial transport of nanotherapeutics.<sup>23</sup> Also, the positively charged collagen and negatively charged hyaluronic acid (HA) can trap charged nanomedicines with high affinity.<sup>24,25</sup>

## 2.2 Alteration in metabolic and immune profiles

Basically, the interior of tumors, particularly their core, presents a hypoxic state, while the surroundings near the vessels are normoxic, which can be explained by the rapid proliferation of tumor cells and deficient oxygen supply from abnormal neovessels.<sup>26</sup> Also, blood vessels exhibit an uneven distribution within tumors, which results in the local hypoxia of tumor regions.<sup>27</sup> Hypoxia can induce the increased expression of hypoxia-induced factors (HIFs)

and stabilize them, subsequently initiating the downstream signalling cascade, such as promoting epithelial-mesenchymal transition, metabolic reprogramming, angiogenesis and resistance to therapy.<sup>28</sup> Metabolic adaption is a key step to satisfy the high energy demand and hypoxia. The change to anaerobic glycolysis alleviates the insufficient oxygen supply and increases lactate production, together with H<sup>+</sup> ions. CO<sub>2</sub> hydration in oxidative tumor areas *via* carbonic anhydrases (CAs) contributes to another part of the production of H<sup>+</sup> ions. These excessive intracellular H<sup>+</sup> ions can be exported *via* Na<sup>+</sup>/H<sup>+</sup> exchangers (NHEs), monocarboxylate transporters (MCTs) and H<sup>+</sup>-ATPases, thus resulting in the acidosis of the TME, tumor proliferation and metastasis.<sup>29,30</sup> Also, tumors increase the production of GSH to cope with the elevated ROS and maintain redox homeostasis. Thus, the above hallmarks can be exploited to develop responsive or TME-modulating therapeutic agents.

In addition, it should be emphasized that another significant feature of the TME is the overall immunosuppressive microenvironment. Immune-infiltrating cells include immunomodulatory cells, such as TAMs, myeloid-derived suppressor cells (MDSCs), regulatory T cells (Tregs) and dendritic cells (DCs), as well as effector immune cells, such as T lymphocytes, B lymphocytes, and natural killer (NK) cells.<sup>31-33</sup> These cells play a dominant and complex role in immune-escape mechanisms. Tumor cells themselves significantly reduce the expression of MHC and upregulate other immunosuppressive molecules, such as programmed death ligand-1 (PD-L1), immune-checkpoint molecules (CD47), and NK-cell ligands (factor associated suicide ligand (FASL)), and recruit anti-inflammatory immune cells.

TAMs represent the main component of myeloid cells, involving pro-inflammatory M1-like phenotype and anti-inflammatory M2-like phenotype, the latter of which is triggered particularly by the hypoxic TME. Within tumors, the predominant M2-like phenotype can facilitate angiogenesis, metastasis and decrease the immune response of T cells.<sup>34</sup> Thus, depleting or switching TAMs can be a potent strategy to reverse immune suppression. Tregs and MDSCs are other partners implicated in the negative modulation of the immune system.<sup>35</sup> Tregs produce TGF- $\beta$  and IL-10 to directly suppress T cell function and release perforin and granzyme to destroy effector T cells, while MDSCs created a large amount of nitric oxide (NO), arginine (Arg)-1 and IL-10, which further decrease the T cell response and promote immunosuppression.<sup>36</sup> The production of indoleamine 2,3 dioxygenase (IDO) can decrease the amino acids (e.g. tryptophan) and recruit Tregs to activate MDSCs, with the aim to suppress T cells. Besides, the immunosuppressive milieu, containing IL-10, TGF- $\beta$ , PD-1 and prostaglandin E (PGE)-2, can reduce the antigen cross-presenting ability of DCs. Also, tumor cells downregulate NK cells to avoid the exposure of TNF-related apoptosis-inducing ligand (TRAIL).<sup>37</sup> The major anti-tumor immune cells in the TME, CD8<sup>+</sup> T cells, are unable to exert an inhibitory response against tumors due to the decreased trafficking into tumor sites (including down-regulation of CD62L on CD8<sup>+</sup> T cells, and the adhesion molecules (ICAM-1 and VCAM-1) and IL-12) and a lack of activation elicited by above immunosuppressive TME.<sup>38</sup> Thus, targeting immune cells or immune-related specific molecules can

reshape the immune microenvironment and boost the efficacy of traditional treatments.

Thus, targeting angiogenesis, the ECM (*e.g.* degrading enzyme and CAFs) and endogenous stimulus-response (*e.g.* hypoxia, pH, GSH and ROS) can enhance the delivery of nanocarriers into tumors and keep the concentrations of drugs within effective therapeutic windows. Besides, modulating the hypoxic, acidic or immunosuppressive microenvironment is another strategy to overcome the dilemma in cancer therapy, and reduce tumor invasion and metastasis (Fig. 1).

### 3. Strategies to overcome the TME barriers

#### 3.1 Strategies for modulating the TME

As mentioned before, the TME dominates the fate of nanocarriers within tumors, from impeding their delivery to resisting conventional therapies.<sup>11</sup> In this section, particular attention is paid to feasible strategies to modulate the TME *via* the following aspects: remodeling the vascular networks, regulating stroma, manipulating hypoxia and pH, and reshaping the immune microenvironment, as summarized in Table 1.

**3.1.1 Remodelling the vascular networks.** Aided by the EPR effect, NPs can passively reach tumors, but their delivery efficiency is relatively low. Thus, to enhance the extravasation of NPs into the TME, there are two opposite strategies based on different rationales, including vascular disruption and vascular normalization.<sup>39</sup>

Vascular disruption was presented as an approach to destroy neovessels, leading to a dramatic decrease in blood supply and the necrosis of tumors. Several vascular disrupting agents such as 5,6-dimethylxanthenone-4-acetic acid (DMXAA) and combretastatin A4 phosphate (CA4P) have verified the practicability of this strategy. After administration, CA4, which is released from CA4P, inhibits tubulin polymerization and destabilizes the cytoskeleton, thus disrupting endothelial cells.<sup>40,41</sup> Chen *et al.* first employed CA4-conjugated poly(L-glutamic acid)-graft-methoxy poly(ethylene glycol) nanodrugs (CA4-NPs) to disrupt vessels, subsequently increasing MMP-9 in tumor tissues. Then, they delivered an MMP9-activated doxorubicin prodrug (Fmoc-GPLGL-DOX), which enhanced the selective release by 3.7-fold.<sup>42</sup> The sequential delivery of CA4-NPs and MMP9-DOX-NPs was a new paradigm for the next generation of tumor-selective enzyme-triggered prodrugs with reduced systemic toxicity. Other research combined this drug with photothermal therapy (PTT), hypoxia-sensitive drug (*e.g.* imiquimod and tirapazamine) and other agents.<sup>43–46</sup> Besides, physical approaches such as radiation, ultrasound, and near infrared (NIR) light treatment can also trigger vascular disruption.<sup>47,48</sup> Tang *et al.* applied  $\alpha_v\beta_3$ -targeting peptide c(RGDfE)-modified hollow copper sulfide NPs to load vinyl azide, which targeted tumor neovasculature and released nitrogen ( $N_2$ ) bubbles under NIR light-induced heating. These bubbles exploded and damaged the neovessels, inducing the ischemic necrosis of tumors, as indicated by photoacoustic imaging.<sup>49</sup>

Vascular normalization has emerged as an alternative to address the biological challenges in delivering NPs. Anti-angiogenic

Table 1 Summary of the TME modulation strategies

| Classification                    | Examples   | Ref.            |
|-----------------------------------|--|-----------------|
| Remodelling the vascular networks | Vascular disruption: DMXAA, CA4P, radiation, ultrasound, and near infrared (NIR) light<br>Vascular normalization: Cediranib, Sunitinib, Bevacizumab, DC101, and NO   | 40–49<br>50–53  |
| Regulating stroma                 | Targeting the ECM:<br>① inhibiting ECM biogenesis: prolyl-4-hydroxylase inhibitor, deferoxamine, and 4-methyl-lumbellifrone<br>② disrupting the ECM: PTT, ultrasound, collagenase, hyaluronidase, cyclopamine, relaxin and NO<br>③ mimicking the ECM: laminin-mimicking peptide  | 56–71           |
|                                   | Targeting CAFs:<br>□ directly disrupting CAFs: FAP-targeting NPs, docetaxel-conjugate nanoparticles or delivering plasmids encoding TNF-related factor<br>□ reducing the activity of CAFs: losartan, quercetin, ellagic acid and dexamethasone   | 72–74 and 77–80 |
| Manipulating hypoxia and pH       | Modulating hypoxia:<br>□ improving blood flow: PTT<br>□ delivering oxygen: hemoglobin and perfluorocarbon<br>□ <i>in situ</i> oxygen production: $MnO_2$ , $CaO_2$ , catalase, and light-driven water splitting<br>□ decreasing oxygen consumption: atovaquone, metformin, tamoxifen, and NO   | 81–92           |
|                                   | Modulating pH:<br>□ neutralizing acidity with buffers: sodium bicarbonate, imidazoles and lysine<br>□ interfering with pH-regulating enzyme: proton-pump inhibitors ( <i>e.g.</i> omeprazole and esomeprazole), MCT inhibitors ( <i>e.g.</i> AZD3965), and CAIX inhibitors ( <i>e.g.</i> sulfonamide- and coumarin-related substances) | 30, 93 and 94   |
| Reshaping immune microenvironment | Targeting immune cells:<br>□ TAMs: CSF-1, bisphosphonates ( <i>e.g.</i> clodronate and zoledronic acid), TLR agonists, chloroquine, celecoxib, NO, and CO<br>□ Tregs: CTLA-4, Sunitinib<br>□ MDSCs: CDDO-Me, 6-thioguanine, and gemcitabine  | 53 and 95–110   |
|                                   | Targeting immune molecules:<br>□ IDO: NLG919 and indoximod<br>□ CXCL12: AMD 3100 or monoclonal antibody  | 111–114         |

drugs, such as Cediranib, Sunitinib, Bevacizumab and DC101, have been shown to decrease vascular leakiness and improve vascular functionality.<sup>50–52</sup> Recently, Chen and coworkers encapsulated  $[\text{Fe}(\mu\text{-SEt})_2(\text{NO})_4]$  (NO donor, DNIC) into lipid-poly(lactic-co-glycolic acid) (PLGA) polymer NPs (NanoNO). After treatment with free DNIC, HUVECs obviously downregulated three pro-angiogenic genes (VEGFA, ANGPT2 and EGF) and increased the expression of two vessel maturation-related genes (S1PR1 and ANGPT1). In contrast with high-dosed NanoNO (1 mg kg<sup>-1</sup>), low-dosed NanoNO (0.1 mg kg<sup>-1</sup>) normalized tumor vessels by increasing pericyte coverage (increased pericyte marker NG2/vessel marker CD31) and functional vessel perfusion (lectin<sup>+</sup>/CD31<sup>+</sup> area increased), thus enhancing the delivery and efficacy of other therapeutics, such as doxorubicin and recombinant TRAIL.<sup>53</sup> More importantly, tumor vessel normalization is closely associated with immunostimulatory pathways, such as lymphocyte infiltration or activity, which provide new route to influence tumor progression.<sup>54</sup> The above low-dosed NanoNO also further evidenced this theory since PD-L1 expression was hampered, anti-tumor M1-like TAMs increased and CD8<sup>+</sup> T cell infiltration was enhanced *in vivo*. This study, for the first time, clearly indicated the difference between low- and high-dosed NO for vessel normalization and the versatility of NO therapy.

However, despite the progress in vascular remodelling, these two strategies have some inevitable drawbacks. For vascular disruption, the abnormal vasculature and impaired lymphatic drainage exacerbate the IFP and hypoxia, further reducing NP penetration and recruiting pro-inflammatory and pro-angiogenic cells. Relatively, vascular normalization increases blood perfusion and mitigates the IFP to promote NP diffusion, but the reduced gaps between endothelial cells may block large-sized NPs.<sup>55</sup>

**3.1.2 Regulating stroma.** After crossing blood vessels, the next formidable barrier is the stroma, which increases solid stress, compresses blood vessels and restricts drug diffusion. Accordingly, two methods have been explored to improve drug delivery, involving modulating the ECM and targeting CAFs.<sup>23</sup>

The ECM can be regulated *via* the following three routes, inhibiting ECM biogenesis, disrupting the ECM and mimicking the ECM. The synthesis of collagen can be interrupted by prolyl-4-hydroxylase inhibitor,<sup>56,57</sup> deferoxamine and siRNA silencing heat shock protein 47,<sup>58</sup> while 4-methylumbelliferon can block the synthesis of HA, another major component.<sup>59,60</sup> Physical methods (*e.g.* PTT and ultrasound<sup>61,62</sup>), enzymes (*e.g.* collagenase and hyaluronidase (HAase)<sup>63–65</sup>) and chemical agents (*e.g.* cyclopamine, relaxin and NO<sup>66–69</sup>) can be applied to facilitate the degradation of the ECM and NP permeation into tumors. Cao *et al.* used NO to trigger MMP expression and disintegrate collagen, which rendered a 2.7-fold greater distribution of mesoporous silica NPs within tumors.<sup>67</sup> However, it should be noted that the above two strategies may increase the chances that tumor cells will migrate and spread throughout the body. By contrast, the final means is based on the fact that cancer cells express ECM degrading enzyme to promote invasion and metastasis. Thus, strengthening the ECM, rather than disrupting it may address tumor metastasis.<sup>70</sup> Considering this, Wang and coworkers constructed a laminin (essential component in

ECM)-mimicking peptide (BP-KLVFFK-GGDGR-YIGSR) (Fig. 2A), where a Y-type RGD-YIGSR motif binding with tumor cells, KLVFF segments, formed the fibrous structure around tumors.<sup>71</sup> This ECM-simulating strategy effectively hampered 82.3% and 50.0% of lung metastasis in breast and melanoma tumor models, respectively, as seen in Fig. 2B–D. This case provided new insight for the inhibition of tumor metastasis.

The subsequent emphasis shifted to ECM origin-CAFs. CAFs are key mediators in the ECM, and contribute to limited drug delivery. Thus, directly disrupting CAFs may improve delivery, and fibroblast activation protein-targeting NPs, docetaxel-conjugate NPs and delivering plasmids encoding TNF-related factor into CAFs were all utilized to verify this hypothesis.<sup>72–74</sup> It is worth noting that direct CAF depletion may promote tumor progression and metastasis, mainly because CAFs possess an anti-tumor phenotype to retard growth.<sup>75,76</sup> Thus, perhaps reducing CAFs activity is a better alternative. There are several anti-inflammatory or anti-fibrotic drugs, such as losartan, quercetin, ellagic acid and dexamethasone.<sup>77–80</sup> If CAFs accidentally internalize therapeutics, this will induce them to secret damage response specific proteins, *e.g.*, Wnt16, which become involved in drug resistance (*e.g.* cisplatin). For example, Huang *et al.* prepared lipid/calcium/phosphate NP-encapsulating quercetin, which greatly downregulated Wnt16 expression, blocked the growth of  $\alpha\text{-SMA}^+$  CAFs and reduced collagen.<sup>78</sup>

**3.1.3 Manipulating hypoxia and pH.** Hypoxia, another significant hallmark of tumors, has recently attracted intense attention because it hinders angiogenesis, metastasis, resistance and failure of other treatments (*e.g.* photodynamic therapy (PDT) and chemotherapy). Several ways exist to improve the hypoxic state, including improving blood flow, delivering oxygen, *in situ* oxygen production and decreasing oxygen consumption.<sup>81</sup> Typically, mild PTT (around 42 °C) can increase blood flow and relieve hypoxia,<sup>82</sup> while delivering oxygen carriers, such as hemoglobin<sup>83</sup> and perfluorocarbon,<sup>84</sup> and also overcome the hypoxia-mediated resistance of tumors towards PDT and radiotherapy. However, the oxygen loading amount is not sufficient to combat hypoxia. Thus, as an alternative, the delivery of agents such as MnO<sub>2</sub>,<sup>85</sup> CaO<sub>2</sub><sup>86</sup> and catalase<sup>87</sup> into tumors can trigger chemical reactions and physical methods, such as light-driven water splitting<sup>88</sup> and *in situ*-produced oxygen, for effective PDT. However, *in situ* oxygen production typically suffers from poor penetration of large NPs, hard-degradable inorganic materials, and low oxygen generation efficiency. Besides increasing the oxygen supply within tumors, inhibiting oxygen consumption provides another potent strategy to alleviate hypoxia. Jiang and coworkers encapsulated verteporfin (PDT agent) and atovaquone into PLGA NPs (ATO/VER NPs), where atovaquone hindered the electron transport of the mitochondria respiratory chain to enhance the PDT efficacy. Under hypoxia, ATO/VER NPs displayed 1.5 times higher cytotoxicity than PDT alone.<sup>89</sup> Metformin,<sup>90</sup> tamoxifen<sup>91</sup> or NO<sup>92</sup> also inhibited the respiratory chain for oxygen-economized PDT, as verified by some studies. This strategy can overcome hypoxia in sparsely vascularized regions and reverse the resistance to oxygen-dependent therapy.

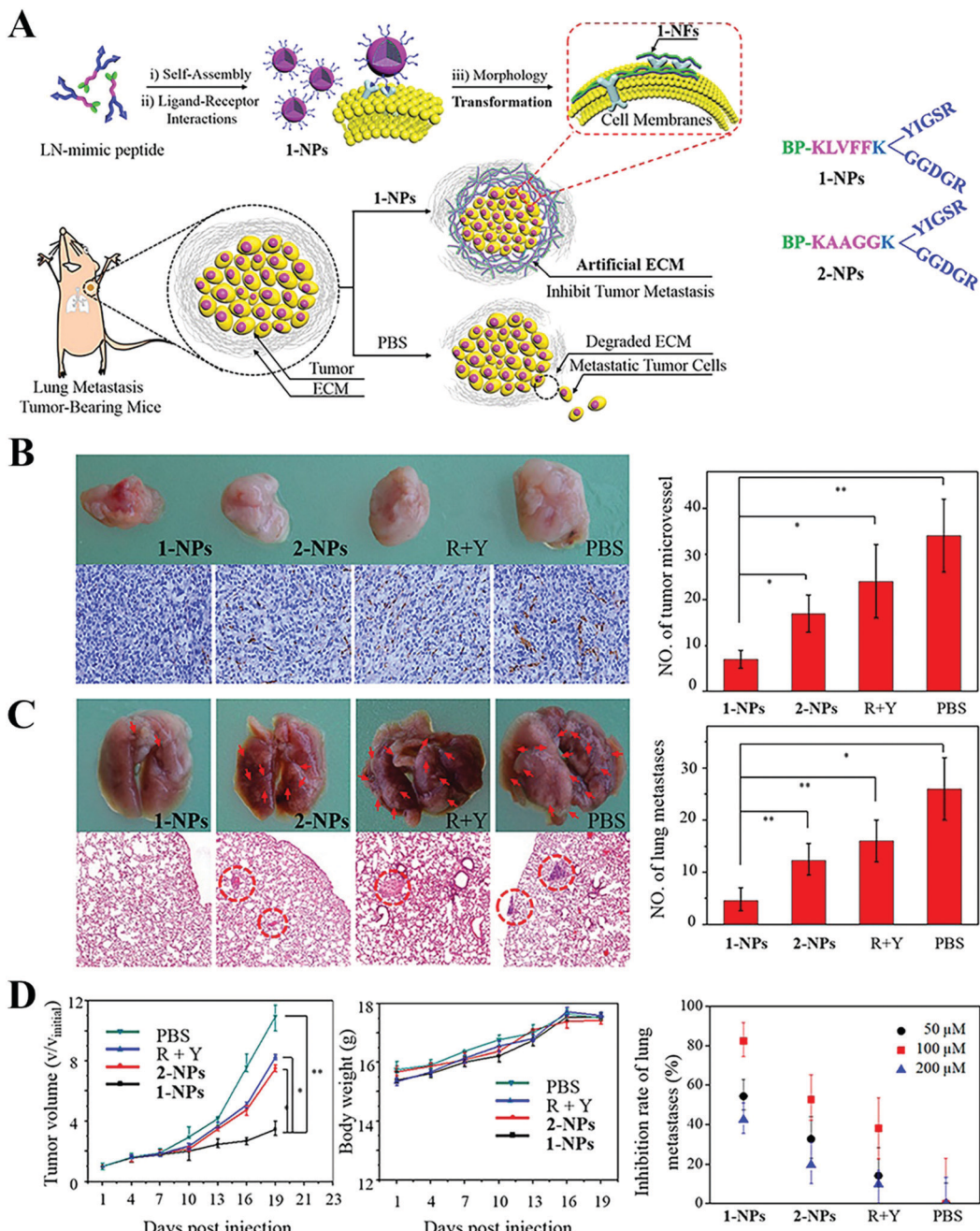


**Fig. 2** Transformable nanomaterials as an artificial extracellular matrix for inhibiting tumor invasion and metastasis. (A) Schematic Illustration. (B) Photos of original tumors (upper panel) and immuno-histochemical staining analyses for CD31 (lower panel) on day 19 after the first administration and the quantitative analysis of MVD (right panel). (C) Photos of the lungs (upper panel) and H&E stained lung slices (lower panel) and quantitative analysis of the lungs (left panel). (D) Tumor volume and body weight of the 1-NPs, 2-NPs, RGD + YIGSR and PBS treated mice and inhibition rate of lung metastases treated with different concentrations of 1-NPs. Data are presented as mean  $\pm$  SD ( $n = 4$ ). \* $p < 0.05$  and \*\* $p < 0.01$ . Reproduced with permission from ref. 71. Copyright © 2017, American Chemical Society.

Hypoxia is usually accompanied by an acidic microenvironment. As discussed earlier, the acidity also contributes to tumor progression and metastasis. The strategies modulating acidosis include neutralizing acidity with buffers and interfering with pH-regulating enzyme.<sup>30</sup> Sodium bicarbonate, imidazoles and lysine were introduced to act as a buffer against acidity and reduce tumor aggressiveness. Proton-pump inhibitors

(e.g. omeprazole and esomeprazole) can inhibit  $\text{H}^+/\text{K}^+$ -ATPase and enhance extracellular pH. The use of MCT inhibitors (e.g. AZD3965<sup>93</sup>), which tackle lactate synthesis-derived  $\text{H}^+$  ions, is another attractive approach to manipulate pH. CAIX expression correlates with the poor prognosis of hypoxic tumors, and thus specific chemical inhibitors (e.g. sulfonamide- and coumarin-related substances) have been employed. Chen *et al.* presented

the self-assembly of a CA inhibitor (benzenesulfonamide)-modified short peptide (N-pepABS), which formed fibrous structures around hypoxic tumor cells triggered by pH, concentrated CA inhibitors on the cell membrane and caused CA dysfunction.<sup>94</sup> N-pepABS regulated the extracellular pH and inhibited cell migration, largely because N-pepABS not only suppresses CAIX enzymes, but its fibrous structure also restricts normal movements for cancer cells. They were also internalised into cancer cells *via* CAIX enzymes and further formed longer fibres in the lysosome, eventually blocking protective autophagy. This study exemplified the effect of regulating CAIX enzymes on acidic pH and hypoxia, while modulating them can reduce the resistance to traditional therapy.

**3.1.4 Reshaping the immune microenvironment.** The aforementioned angiogenesis, stroma, hypoxia and pH modulation generally convert the intrinsic immunosuppression into immunostimulatory, which confers better therapeutic outcomes in combination with immunotherapy. Thus, in this section, targeting immunosuppressive factors, involving cells or soluble mediators, is the main focus of our discussion.

Negative regulatory cells include TAMs, Tregs and MDSCs, which inhibit the anti-tumor immune response of T cells and NK cells. M2-like TAMs secret some immunosuppressive cytokines, such as IL-10, PGE-2 and TGF- $\beta$ , and small amounts of proinflammatory cytokines (IL-6, TNF- $\alpha$ ), resulting in evasion-mediated immune suppression.<sup>32</sup> Colony-stimulating factor 1 receptor (CSF-1R) or bisphosphonates (*e.g.* clodronate and zoledronic acid) can directly inhibit the survival and proliferation of macrophages. However, the direct depletion of TAMs can kill M1-like macrophages, and thus researchers have modified several ligands to enhance the M2-targeting ability, such as M2pep and anti-CD204 immunotoxin.<sup>95</sup> Reprogramming TAMs into an M1-like phenotype represents a relatively ideal method based on the excellent plasticity of macrophages. Metal NPs, such as gold, silver and iron oxide, can increase ROS within TAMs, thus activating M1-like macrophages.<sup>96,97</sup> Several therapeutics also mediated this switching, such as TLR agonists,<sup>98</sup> chemicals (chloroquine and celecoxib<sup>99,100</sup>), and gases (NO and CO<sup>53,101</sup>). For example, Yao *et al.* fabricated two look-like nanodrugs (GLnano), which were both established on anti-angiogenic low molecular weight heparin (LMWH), and mixed together to administer to mice for melanoma treatment.<sup>102</sup> One of the nanodrugs was doxorubicin (DOX)-loaded LMWH-chrysin (LCY) with DSPE-PEG-anisamide decoration (D-LCA nanodrugs) to actively kill tumor cells. The other was celecoxib-loaded LMWH-PLGLAG-containing peptide conjugation (C-Lpep), which could release celecoxib for M2-to-M1-like macrophage reeducation. This GLnano effectively inhibited tumor growth, and on day 10, the tumor size was only 1/2, 1/4, and 1/8 of that in the D-LCA, free DOX, and saline groups, respectively. For Tregs, the strategies can also be divided into three types, including depletion<sup>103,104</sup> (using PDT or chemotherapy), function inhibition with anti-cytotoxic T-lymphocyte-associated protein 4 (CTLA-4) molecules and modulating Tregs by the signal transducer and activator of the transcription (STAT)3/5 pathway.<sup>105</sup> Some studies revealed STAT3 of immune

cells facilitate secretion of Th2 cytokines, thus suppressing the Th1 response and promoting the survival of Tregs.<sup>106</sup> Sunitinib, a tyrosine kinase inhibitor, acts on this pathway and lowers the proportion of Tregs and MDSCs.<sup>107</sup> In the case of MDSCs, derivatives of oleanolic acid (CDDO-Me),<sup>108</sup> 6-thioguanine<sup>109</sup> and gemcitabine<sup>110</sup> all were used to inhibit their function and development.

Besides targeting immune cells, soluble mediators such as IDO, MMP, TGF- $\beta$  and CXCL12 play a vital role in promoting the immunosuppressive microenvironment. Thus, delivery of these mediator-related inhibitors is viewed as a viable approach to regulate the immune system. IDO can catalyze the degradation of tryptophan to kynurenine, and a low concentration of tryptophan impairs the survival and activity of cytotoxic T cells. IDO inhibitors such as NLG919 and indoximod with the use of nanocarriers exert an effective immune response against tumors, in combination with other treatments.<sup>111–113</sup> Notably, IDO inhibitors alone cannot induce an intense immunostimulatory response. Wang *et al.* fabricated redox-responsive phospholipid-porphyrin conjugates to self-assemble into liposomes (IND@RAL), in which NLG-8189 was loaded in their lumen (Fig. 3A).<sup>111</sup> After tumor cell internalization, IND@RAL responded to the high GSH levels in the tumor cells, then recovered the fluorescence signal and PDT activity (>100-fold). Strikingly, GSH-activated PDT induced immunogenic cell death at the primary tumor sites and recruited CD8 $^{+}$  T cells into the tumors. After combination with IDO inhibitor, the systemic antitumor immune response was further enhanced, as evidenced by the inhibition of metastatic sites (Fig. 3B). Tumor cells and mesenchymal cells secret chemokines (*e.g.* CXCL12) to activate and recruit immunosuppressive cells, such as Tregs, into the TME. Small-molecule inhibitors (AMD 3100) or monoclonal antibody can block this effect of CXCL12.<sup>114</sup>

### 3.2 Strategies for tumor active targeting

Besides TEM modulation, physical NPs feature, such as size, surface chemistry, shape and existence of targeting ligands, can also influence the tumor distribution and cellular uptake of NPs. In this section, we focus on how to enhance targeting capacity towards tumors or non-cancer cells in the TME for improved delivery and efficacy, including the modifying targeting ligand and biomimetic strategy, as depicted in Fig. 5.

**3.2.1 Targeting ligand modification.** Targeting ligand modification is one of the widely used strategies to improve the tumor targeting delivery of NPs, which is attributed to the specific interaction between ligands on NPs and proteins on the membrane of tumor cells or tumor stroma cells.<sup>115</sup>

Initially, researchers attempted to use some natural ligands that could recognize proteins overexpressed on tumor cells or stromal cells. For example, transferrin is the most widely used ligand, which can specifically interact with transferrin receptor (TfR) overexpressed on tumor cells and endothelial cells.<sup>116</sup> Also, oxaliplatin-loaded transferrin-modified liposomes are under clinical evaluation. Although high tumor selectivity and therapeutic activity were observed in the pre-clinical study, thrombocytopenia was found as the main toxicity in the Phase I study.<sup>117</sup>

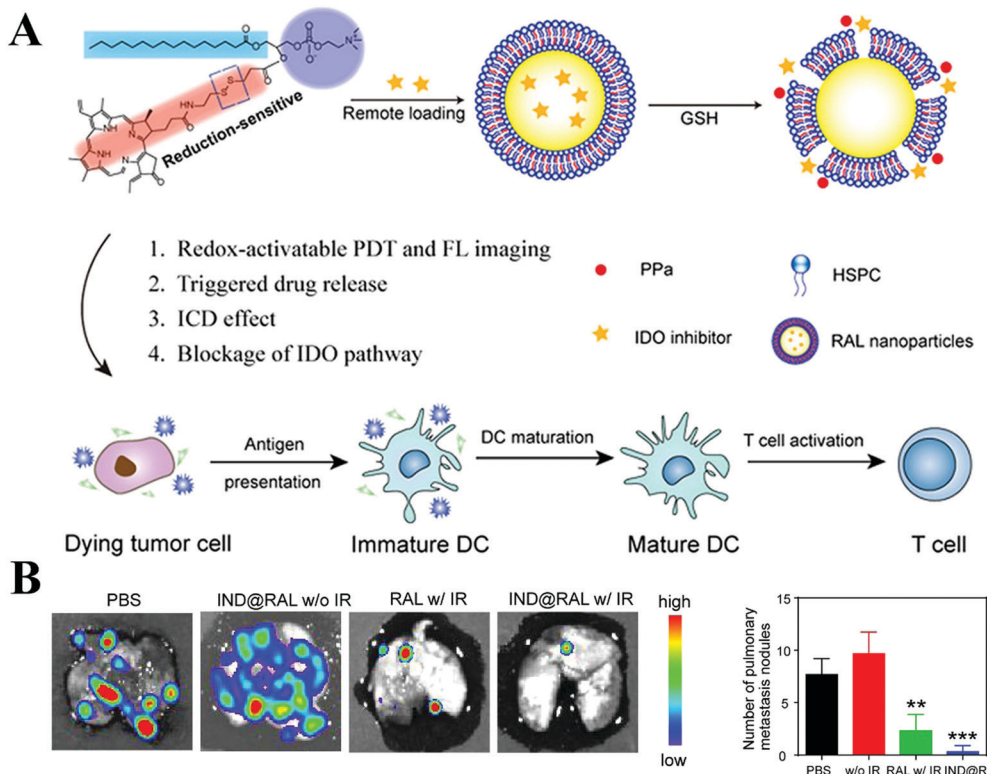


**Fig. 3** Porphyrin-based liposome loaded with IDO inhibitor for synergistic photoimmunotherapy. (A) Schematic Illustration. (B) Antimetastasis of each group imaged by BLI analysis (left panel) and the number of lung metastatic nodules of mice bearing 4T1-Luc tumors at the end of the antitumor study (right panel). Reproduced with permission from ref. 111. Copyright © 2019, American Chemical Society.

Additionally, the most serious limitations of proteins as targeting ligands are their poor stability, large molecular weight, high immunogenicity, and high cost,<sup>118</sup> which restrict the application and clinical translation of protein-decorated NPs.

To solve the above-mentioned problems, peptides with several or tens of amino acids in length were designed for tumor targeting.<sup>119</sup> T7 peptide (HAIYPRH) is one such ligand that can specifically bind with TfR.<sup>120</sup> However, the traditional L-form peptide still suffers from quick degradation by enzymes in the blood, while the retro-inverso D-form peptide was still integral after 8 h incubation.<sup>121</sup> Additionally, D-form T7 peptide (D-T7) showed stronger binding affinity with TfR compared with L-formed T7.<sup>122</sup> Thus, we conjugated D-T7 onto PEGylated bilirubin nanoparticles (BRNPs) for brain tumor targeting delivery.<sup>123</sup> The results showed the brain tumor accumulation of D-T7-modified BRNPs (TBRNPs) was over 4-fold higher than that of BRNPs (Fig. 4A–C). According to the fluorescence distribution in the brain slices (Fig. 4D and E), the TBRNPs showed higher intensity in the brain tumor, and well co-localized with TfR, indicating the TfR-mediated active targeting of TBRNPs. Cediranib-loaded TBRNPs could better target neovessels and inhibit the tyrosine kinase activity of c-KIT and VEGFR1, 2 and 3 for anti-angiogenesis. As a result, cediranib and paclitaxel-loaded TBRNPs greatly prolonged the medium survival time of brain tumor-bearing mice from 16 days to 53 days, which was significantly longer than that for the unmodified BRNPs. Also, there are several other targeting

ligands for tumors or other cells in the TME, such as RGD (targeting vascular receptor Integrin  $\alpha_v\beta_3$ <sup>49</sup>), fibroblast activation protein antibody (targeting CAF),<sup>124</sup> vitamin D ligand (targeting CAFs in pancreas),<sup>125</sup> and mannose (targeting DCs<sup>126</sup> or cancer cells<sup>127</sup>).

**3.2.2 Biomimetic NPs.** In the body, circulating cells, such as platelets, circulating tumor cells and macrophages, can target tumor with high efficiency. Thus, biomimetic NPs coated with these cell membranes,<sup>128</sup> drugs and NPs-loaded cells or exosomes can mimic the interaction among these cells or between stromal cells and cancer cells, such as cell recruitment and immune escaping, to improve the delivery and efficacy of drugs. For example, the vascular disruption in tumors can recruit platelets in the blood and cause coagulation.<sup>129</sup> Therefore, Zhang *et al.* coated a platelet membrane onto mesoporous silica NPs (MSNs), which were loaded with hypoxia activated tirapazamine (TPZ) and vasculature-disruptive agent DMXAA for tumor treatment.<sup>130</sup> The designed particles, MTD@P, showed good selectivity to cancer cells. Compared with the normal cell line 3T3, the uptake of MTD@P in the colon cancer cell line CT26 increased 15 times. After entering the tumor, MTD@P could disrupt the tumor vasculature to inhibit tumor growth. Glycoprotein VI (GPVI) on platelet membranes is vital for the recruitment of platelets toward injured vascular sites, which exposes the vascular epithelial collagen to bind with GPVI.<sup>131</sup> Thus, the vasculature disruption recruited more platelet-mimic MTD@P, reinforcing its hypoxia and TPZ

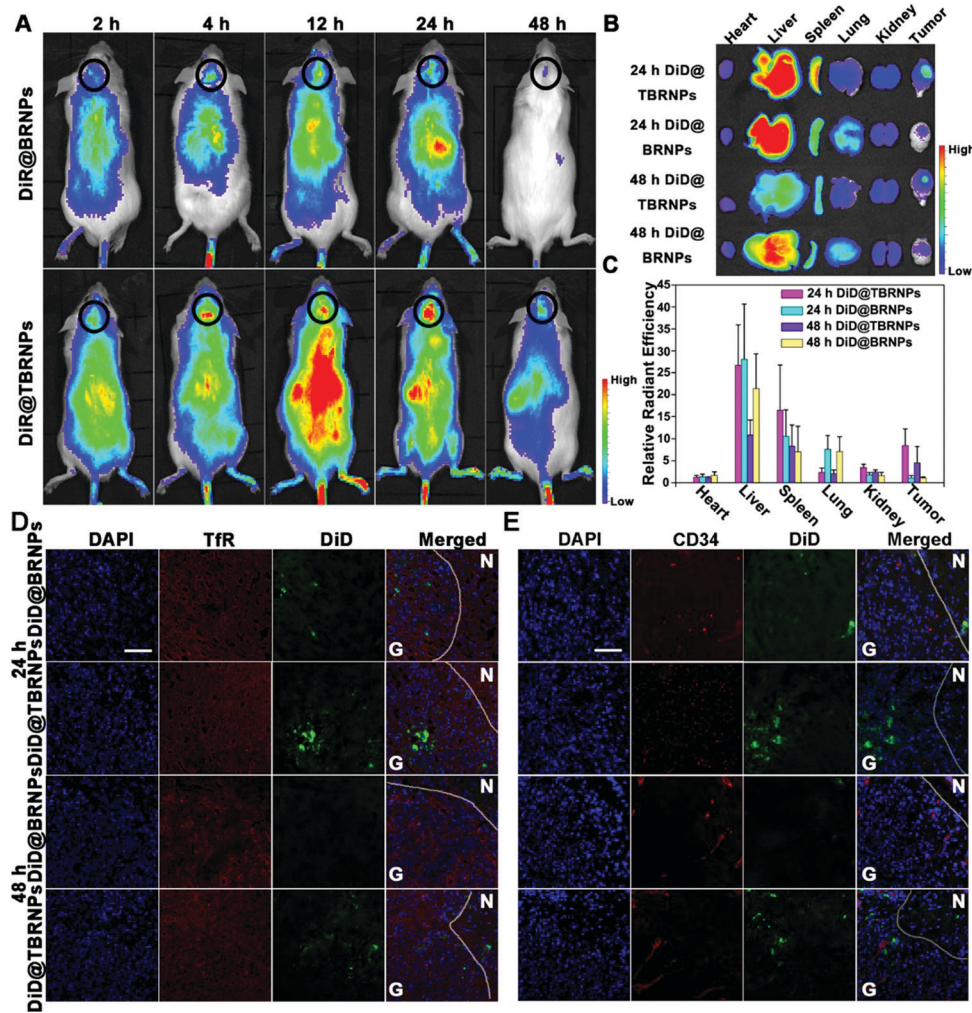


**Fig. 4** Fluorescence distribution *in vivo*. (A) Fluorescence signal distribution of different nanoparticles with the extension of time *in vivo*. Bar represents radiant efficiency between 1935 and 6154. (B) Fluorescent imaging of organs *ex vivo*. Bar represents radiant efficiency between  $8.26 \times 10^7$  and  $3.11 \times 10^9$ . (C) Semi-quantification of the fluorescence signals. (D and E) Fluorescence distribution of DiD@BRNPs and DiD@TBRNPs in glioma sections after intravenous injection at 24 h and 48 h, where green indicates DiD, blue indicates nucleus and red indicates TfR and CD34, respectively. N represents the normal brain, G represents the glioma, and bars represent 50  $\mu$ m. Reproduced with permission from ref. 123. Copyright © 2019, American Chemical Society.

efficacy. Macrophages also display tumor targeting capacity.<sup>132</sup> Our group coated a shape-changeable NP with a macrophage membrane to improve its targeting capacity, and encapsulated thioketal-linked PTX dimer and disulfide-linked IND dimer for the combination of chemotherapy and immunotherapy.<sup>133</sup> The coated NPs, I-P@NPs@M, showed higher cellular uptake by cancer cells and IDO overexpressed cells compared with that of the uncoated NPs I-P@NPs. *In vivo*, I-P@NPs@M showed 1.38-fold higher intensity in 4T1 breast tumor than I-P@NPs.

Directly loading NPs or drugs into whole cells can also achieve active tumor targeting. Xue *et al.* used neutrophils to deliver paclitaxel-loaded liposomes (PTX-CL/NEs) for glioma recurrence treatment.<sup>134</sup> After surgical removal of a glioma, local brain inflammation occurs accompanied with the release of inflammatory factors, such as TNF $\alpha$ , which can activate neutrophils to migrate to the inflammatory area.<sup>135</sup> Compared with paclitaxel-loaded liposomes (PTX-CL), the blood brain

barrier penetration ratio of PTX-CL/NEs increased from 1% to 38%, while the penetration into glioma spheroids by PTX-CL/NEs also increased significantly. Similarly, macrophages also show potential as carriers of drugs and NPs for tumor targeting delivery.<sup>136</sup> Guo *et al.* loaded doxorubicin into M1 macrophages (M1-Dox) for the treatment of metastatic ovarian carcinoma.<sup>137</sup> When M1-Dox interacted with the tumor cells, it formed tunnelling nanotubes to transport doxorubicin from the macrophages to tumor cells, providing an effective drug transportation pathway and leading to an effective antitumor effect.

Similarly, exosomes and vesicles can serve as drug carriers due to their long blood circulation time, immune escape and potential tumor targeting.<sup>138</sup> Wang *et al.* loaded doxorubicin into macrophage-derived exosomes and then modified them with gold nanorods.<sup>139</sup> After entering the tumor, the photothermal effect of the gold nanorods caused disruption of the exosomes and they released doxorubicin, boosting enhanced

chemo-photothermal combinational therapy. Furthermore, some exosomes may directly kill tumor cells. A recent study showed engineered T cells expressing chimeric antigen receptor (CAR) could release exosomes, which also carried CAR on their surface.<sup>140</sup> As a result, the cytotoxic molecule-expressed CAR-T cell exosomes could directly inhibit tumor growth. Additionally, the CAR exosomes did not express PD1, making them safer than CAR-T therapy.

Besides mimicking biological components in the body, the immune system can also be hitchhiked for tumor targeting delivery. Li *et al.* developed a type of cisplatin loaded nano-pathogenoid,<sup>141</sup> which could *in situ* hitchhike circulating neutrophils. When the tumor was applied with PTT, PTT-induced inflammation recruited neutrophils together with the nano-pathogenoid. The inflammation factors in the tumor caused the release of the nano-pathogenoid from the neutrophils, which were then taken up by tumor cells. Finally, the cisplatin in the nano-pathogenoid led to apoptosis of the tumor cells. Thus, this hitchhiking strategy can effectively target tumors with a simple NP composition and preparation, which is promising for clinical translation.

### 3.3 Strategies for TME-responsive drug delivery

Compared to normal tissue, the unique characteristics of the TME, including low pH, hypoxia, and high levels of redox potential and enzymes, have guided the construction of stimuli-responsive NPs.<sup>142</sup> Generally, the pre-designed functions of these NPs can be activated in response to the TME signals, as shown in Fig. 6, such as detachment of the PEG corona, surface charge conversion, ligand exposure, and on demand drug release, for enhanced deep tumor penetration, augmented drug release, and increased tumor cell uptake.<sup>143–146</sup> Based on these strategies, the efficacy of TME-triggered cancer treatment has greatly improved.

**3.3.1 Enhanced tumor penetration of NPs.** Initial tumor accumulation of drug carriers is a critical step for tumor therapy. To date, studies mainly focus on stimuli-responsive

modulation of the physiochemical properties of particles, such as particle size, shape, surface charge, and ligand presence.<sup>147–149</sup> The challenges associated with particle size is well-known. Firstly, the pores between endothelial cells range from 200 nm to 1.2  $\mu$ m in size, depending on the tumor type. Secondly, after extravasation from vessels, NPs with a larger size ( $>100$  nm) are more likely to be retained in the TME but it is difficult for them to penetrate within the tumor due to the dense ECM, whereas smaller NPs ( $<30$  nm) can penetrate into the deeper region of tumor, but be easily pumped back into the bloodstream by the high IFP.<sup>150</sup> Based on this, the development of size-shrinkage platforms is necessary. Briefly, after blood circulation, particles with a relatively large size can respond to internal stimuli, such as enzymes,<sup>151</sup> acidic pH,<sup>152</sup> and hypoxia,<sup>153</sup> to achieve size shrinkage and tumor penetration.<sup>154</sup>

The first strategy has been established on the principle that TME cues will induce the detachment or degradation of the outer shell layer on NPs. In this regard, many studies have been devoted to design NPs with matrix metalloproteinase (MMP)-sensitive peptides or benzoic imine-conjugated PEG corona,<sup>155,156</sup> which can respond to either a higher expression level of MMP or lower pH at the tumor site to form smaller NPs. These size-shrinkage characteristics result in improved penetration into the tumor site due to the easier diffusion throughout the tumor interstitial space. In addition, tethering small particles on the surface of other NPs or hiding them inside large particles through TME-sensitive linkers can also prompt the penetration of small NPs when the platform is exposed to the TME.<sup>157–160</sup> Cui *et al.* fabricated P-DOX by conjugating doxorubicin (DOX) with poly(4-formylphenyl methacrylate-*co*-2-(diethylamino)ethyl methacrylate)-*b*-poly(ethylene glycol) methacrylate) (P(FPMA-*co*-DEA)-*b*-POEGMA) *via* imine linkage.<sup>161</sup> The constructed pH sensitive NPs could dissociate into ultrasmall particles ( $\sim 10$  nm), which are inherently favorable for deep tumor penetration.

Objectively, the deep penetration efficacy of any of the abovementioned methods will not be perfect due to the complexity of the TME. Hence, the combination of multiple strategies, including the modulation of NP properties (size shrinkage/surface charge conversion) and remodeling the TME, has become a promising approach to improve the penetration capacity.<sup>162,163</sup> In addition, TME-triggered self-assembled NP can also be used to improve solid-tumor penetration. For instance, Wang *et al.*<sup>164</sup> employed an *in vivo* self-assembly strategy and designed polymer-peptide conjugates (PPCs), which underwent an increase in acid-induced hydrophobicity under a narrow pH-response range. The results showed that at appropriate molecular concentrations (around the IC<sub>50</sub> values of PPCs), *in situ* self-assembly in the TME enabled the drug to be delivered deeper into the tumor.

**3.3.2 Increased cellular uptake of NPs.** TME-responsive NPs with charge conversion and shell detachment can also be utilized as advanced strategies for tumor-specific cellular uptake, which can offer several advantages, such as solving the dilemma of long blood circulation (negative charge) and efficient cellular uptake (positive charge). Some TME cues, such

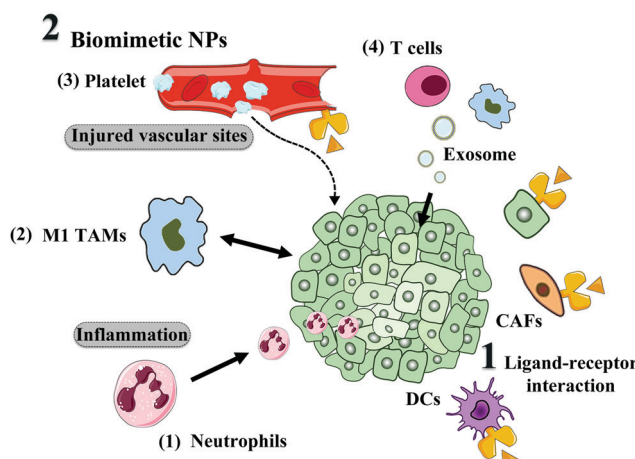


Fig. 5 TME and tumor cell active targeting, including ligand modification and biomimetic strategies.

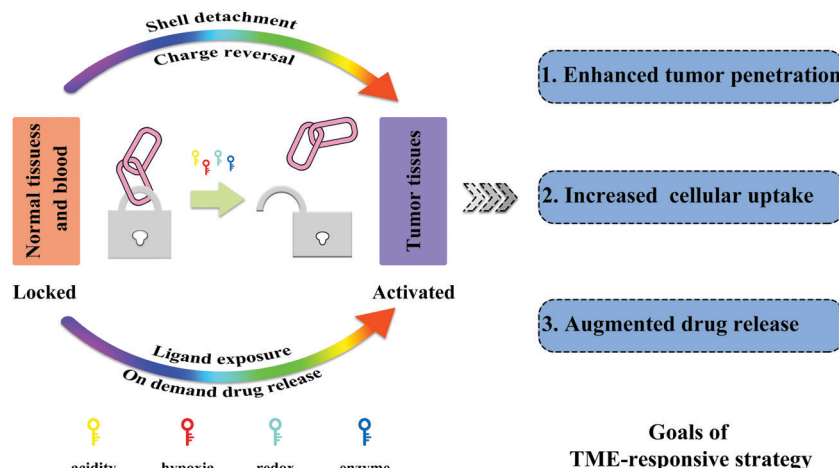


Fig. 6 Size, charge, and ligand availability modifications to sequentially take advantage of favorable physicochemical properties during systemic circulation and tumor penetration.

as redox potential, acidic pH, and overexpressed enzymes, can stimulate the responsive bonds on the surface of NPs to achieve charge reversal.<sup>165,166</sup> For example, ionizable chemical groups (amine and acyl sulfonamide) and pH-cleavable chemical bonds (hydrazone, imine, and dimethyl maleic anhydride) are commonly used as pH-sensitive linkers.<sup>167</sup> Similarly, quaternary amine bonds are charge switchable, which can be protonated at weak acidic pH to improve the cellular uptake of NPs.<sup>168</sup>

In addition, TME signals can target the sensitive bonds on NPs to recover hidden ligands, and thus achieve enhanced tumor internalization. Generally, targeting ligands should be shielded during the blood circulation to circumvent their non-specific interaction with surrounding healthy tissue. One effective approach to achieve this purpose utilizes enzyme- and pH-sensitive PEG coatings. The overexpressed enzymes in the TME can cleave bonds (*e.g.* MMP-2 and MMP-9) to deshield PEG and expose the targeting ligands to promote efficient cellular uptake. In their pioneering research article, Ji *et al.* constructed enzyme-sensitive GEM nanovectors through the conjugation of matrix metalloproteinase-9 (MMP-9) detachable PEG (Fig. 7A).<sup>169</sup> When the nanovectors accumulate at the tumor site *via* the EPR effect, the PEG corona can be detached through overexpressed MMP-9 to expose RGD for facilitating cellular internalization, as seen in Fig. 7B.

**3.3.3 Augmented drug release at tumor site.** TME cues can trigger a hydrophilic-hydrophobic switch, leading to the collapse of NPs and on demand drug release. For example, pH-sensitive NPs are fabricated with polymers that switch between the hydrophilic (swollen) and hydrophobic (collapsed) states as a result of the protonation and deprotonation of their functional groups (*e.g.* poly(2-(diisopropylamino)ethyl methacrylate) (PDPA)) to trigger drug release.<sup>170</sup>

Besides, cleaving various TME-sensitive linkers to degrade NPs is another strategy for the efficient release of loaded therapeutics. Recently, hypoxia-mediated drug release has aroused attention, in which hypoxia-responsive molecules such as nitroimidazole (NI) are incorporated into NPs. When exposed

to the tumor hypoxic environment, hydrophobic NI segments are converted into hydrophilic 2-aminoimidazole, thereby facilitating the release of the drug encapsulated in NPs.<sup>171</sup> Furthermore, azobenzene (AZO), as a hypoxia-sensitive linker, can also be used to conjugate carboxymethyl dextran (CMD) with black hole quencher 3 (BHQ3) to load DOX. When these particles enter the hypoxic tumor site, the release rate of DOX remarkably increases through the cleavage of the azo bond in BHQ3.<sup>172</sup> In addition, redox-sensitive linkages, including disulfide (S-S) and diselenide (Se-Se) linkers, are integrated into the backbone or side chains to attain redox-sensitive drug release.<sup>173</sup>

Notably, the acidic pH in the TME can induce the collapse of some inorganic NPs, such as manganese dioxide ( $MnO_2$ ), calcium carbonate ( $CaCO_3$ ) and calcium phosphates ( $Ca_3(PO_4)_2$ ) by facilitating the release of loaded cargo.<sup>174</sup> Additionally, the utilization of TME signals to trigger the generation of gas (*e.g.*  $CO_2$  and  $H_2S$ ) demonstrates great potential for accelerated drug release.<sup>175</sup>

## 4. Challenges of overcoming TME barriers

Based on the distinguished TME, many types of TME-modulating strategies and NPs have been developed to overcome the biological barriers and improve drug delivery efficiency. However, although impressive progress has been made, there are still many issues remaining to be elucidated and improved.

### 4.1 Cross talk of the complex TME

The complex properties of the TME construct a network in which the alteration in a specific character will influence many other characters. As described above, angiogenesis is an important character of tumors, resulting in leaky vasculature and EPR effect, where the latter is the most widely accepted rationale for designing nanoscale drug delivery systems.<sup>176</sup> However, the leaky vasculature also leads to extravasation of blood components,

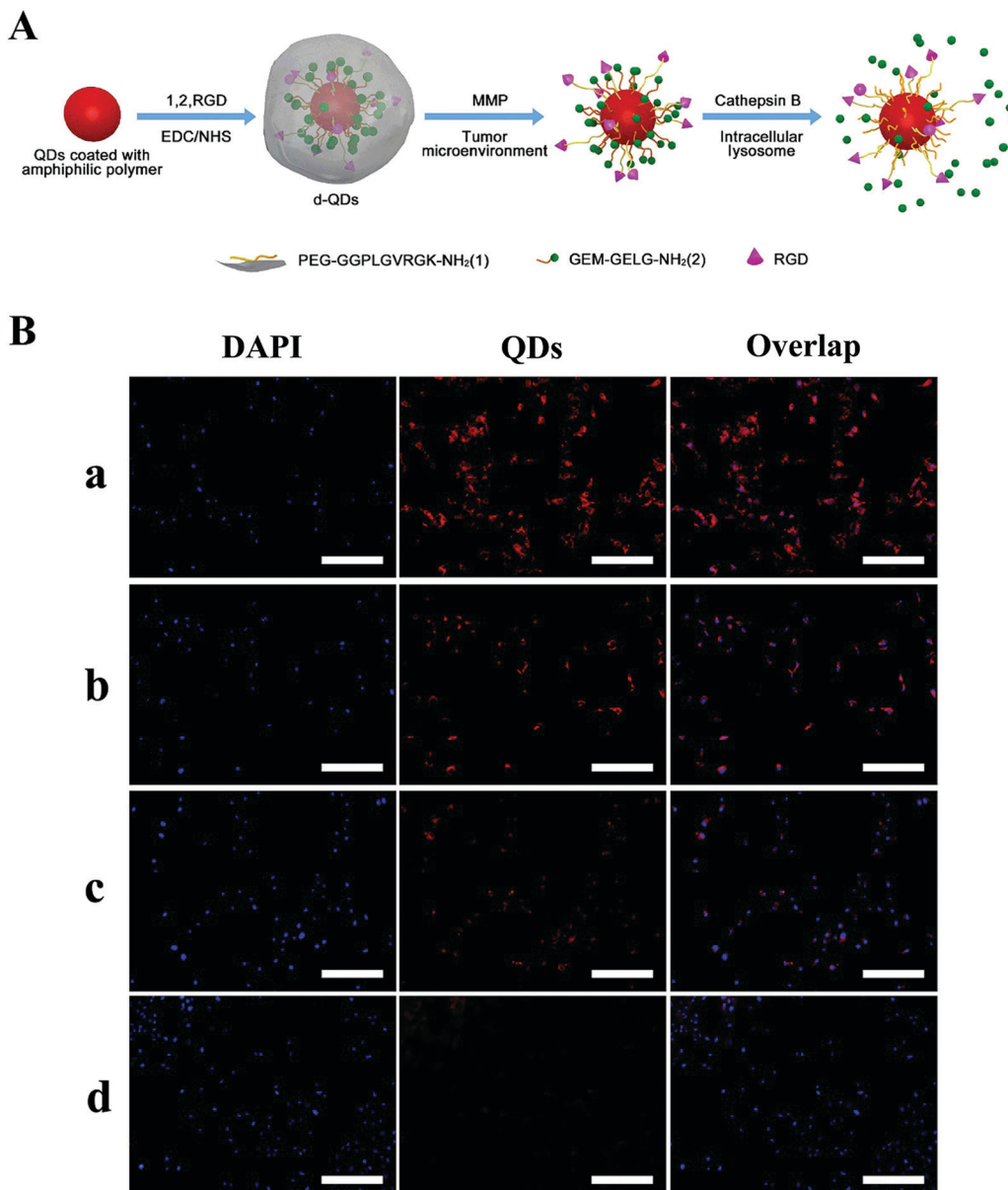


Fig. 7 Dual enzymatic reaction-assisted GEM nanovectors achieving multistage tumor cell targeting and efficient drug release. (A) Schematic illustration of the preparation of the nanovectors and their enzyme-sensitive behavior. (B) Fluorescence microscopy images of BxPC-3 cells incubated with d-QDs in the (a) absence and (b) presence of the MMP inhibitor, (c) cb-QDs (cathepsin B-sensitive QDs without MMP-9 responsiveness, with an uncleavable PEG shell), and (d) d-QDs (nr) (dual-enzyme-sensitive QDs without RGD targeting ability) with a concentration of 200 nM QDs for 4 h. The scale bar is 200  $\mu$ m. Reproduced with permission from ref. 169. Copyright © 2017, American Chemical Society.

such as proteins, resulting in high IFP, and finally inhibits the passive diffusion of drugs and NPs. Therefore, many researchers have developed tumor vessel normalization strategies by anti-angiogenesis to reduce IFP and improve the penetration of NPs.<sup>11</sup> Although these studies have reported enhanced drug delivery and antitumor effect, anti-angiogenesis greatly reduces blood perfusion of tumors, which aggravates the deficiency of oxygen in tumors, and unfortunately, hypoxia is considered as a contributor to tumor resistance towards chemotherapy.

Similarly, inhibition of the tumor matrix synthesis can reduce the density of the tumor matrix, which can improve tumor penetration. For example, oral administration of losartan can

apparently reduce the synthesis of collagen *via* recognition of the angiotensin II type I receptor, which can downregulate tumor transforming growth factor- $\beta$ 1.<sup>177</sup> Thus, the combination of oral losartan with NPs can improve the tumor targeting delivery of NPs.<sup>178</sup> However, the loose tumor matrix also facilitates the extravasation of tumor cells, which will elevate metastasis potential. Unfortunately, most studies do not pay much attention to this concern.

#### 4.2 Active targeting and cell uptake

Ligand modification is the most widely used strategy to overcome tumor biological barriers, improve tumor active targeting

and facilitate cell uptake.<sup>115</sup> Although the targeting capacity of ligands has been widely accepted, and some ligand-modified nanomedicines are under clinical evaluation, the efficacy of ligand modification is challenged by the formation of a protein corona.<sup>179</sup> Upon interaction with biological fluid, proteins in the fluid can adsorb on NPs and form a protein layer, called the protein corona. Several studies indicate that the formation of a protein corona may diminish or even eliminate the specific interaction of a ligand with its receptors, while some studies indicate the specific interaction is still reserved in *in vivo* conditions.<sup>180,181</sup> However, regardless if the targeting is diminished or eliminated, the protein corona indeed influences the active targeting and cellular uptake of NPs. Therefore, it is useful to develop strategies that can overcome the influence of the protein corona.

Surface de-shielding may be an applicable strategy to overcome the influence of the protein corona. A PEG layer on the surface of NPs can reduce the adsorption of protein and improve the blood circulation time, and thus PEGylation is widely used in the construction of drug delivery systems.<sup>182</sup> However, the PEG layer also inhibits the interaction between NPs and cells. Therefore, PEG should be conjugated onto NPs through a cleavable linker.<sup>183</sup> When the NPs arrive at the tumor, specific stimuli, such as acidic condition and overexpressed enzyme, will trigger the detachment of PEG from the NPs and the protein corona will be detached correspondingly, resulting in the exposure of the inner ligand on the NPs and specific targeting to tumor cells.<sup>184</sup>

#### 4.3 Specificity and efficiency of stimulus response

Responsive drug delivery systems are designed in response to the stimuli in tumors to improve drug delivery, such as acidic condition, GSH, ROS and overexpressed enzymes. Thus, it is important to ensure the response occurs in the right location, the tumor. Although the conditions in the tumor are different compared with that of other tissues, they indeed exist in normal tissues. For example, the concentration of GSH in tumor cells, especially in the cytoplasm, may be as high as 1–10 mM, which can be used for designing GSH-sensitive drug delivery systems.<sup>185</sup> However, GSH is distributed throughout the body. The concentration of GSH in the blood is about 2–20 µM, which is the first place that NPs enter after intravenous injection. Due to the long time that NPs circulate in the blood, it is important to prohibit premature drug release in response to GSH. Thus, to circumvent this problem, dual-responsive drug delivery systems have been designed, where the effective response requires the existence of two stimuli.<sup>186</sup>

Besides the responsive specificity, responsive efficiency is another important issue. Although NPs display an enhanced retention effect compared with free drugs, their retention time in tumors is still limited, with a half-life of several hours. Therefore, NPs should respond to stimuli as quickly and efficiently as possible before they are cleared from the tumor. Although the degrading reaction of specific substrates by enzymes is very rapid, the full response of NPs is time-consuming. For example, gelatin NPs incubated with MMP-2 were reduced

only to half of their initial size in about 8 h.<sup>187</sup> Unfortunately, more than half of the NPs will be pumped back into the blood within 8 h. This time-consuming procedure may explain the limited benefit of enzyme-sensitive drug delivery system.

## 5. Conclusion

The knowledge about the barriers in the TME for drug delivery have been greatly extended. In the present review, we summarized the knowledge about the barriers, and then discussed the strategies to overcome these barriers and improve drug delivery. Although promising development has been made in this area, there are still some issues that need to be given great attention. In addition to the challenges discussed in last section, the properties of NPs are also very important. There are numerous studies that show the surface moieties, charge, size, shape, softness and even the inner core of NPs can influence their behaviour. This means there is no general rule that all NPs obey. Thus, case-by-case evaluation should be performed before obtaining a good drug delivery system. The safety of drug delivery systems is another critical concern. Although the strategies in this review showed the potential of improving drug delivery to tumors, most NPs, at least over 90%, will go to normal tissues. Thus, biocompatible and biodegradable materials should be used in the construction of drug delivery systems. Recently, some carrier-free NPs have been developed with tumor targeting capacity. Due to the termination of the use of toxic materials, carrier-free NPs hold great promise in clinical application.

In short, great improvement has been made in TME-targeting drug delivery. A better understanding about the TME will further improve the drug delivery efficiency and antitumor outcome.

## Conflicts of interest

The authors declare no conflict of interest.

## Acknowledgements

The work was supported by National Natural Science Foundation of China (81961138009), Research Funds of Sichuan Science and Technology Department (19YYJC2250), 111 Project (B18035) and the Fundamental of Research Funds for the Central Universities.

## References

- 1 F. Bray, J. Ferlay, I. Soerjomataram, R. L. Siegel, L. A. Torre and A. Jemal, *Ca-Cancer J. Clin.*, 2018, **68**, 394–424.
- 2 World Health Organization. Cancer, <https://www.who.int/health-topics/cancer>.
- 3 M. Björnalm, K. J. Thurecht, M. Michael, A. M. Scott and F. Caruso, *ACS Nano*, 2017, **11**, 9594–9613.
- 4 D. Peer, J. M. Karp, S. Hong, O. C. Farokhzad, R. Margalit and R. Langer, *Nat. Nanotechnol.*, 2007, **2**, 751–760.

5 R. van der Meel, E. Sulheim, Y. Shi, F. Kiessling, W. J. M. Mulder and T. Lammers, *Nat. Nanotechnol.*, 2019, **14**, 1007–1017.

6 J. W. Nichols and Y. H. Bae, *J. Controlled Release*, 2014, **190**, 451–464.

7 Y. S. Youn and Y. H. Bae, *Adv. Drug Delivery Rev.*, 2018, **130**, 3–11.

8 J. Shi, P. W. Kantoff, R. Wooster and O. C. Farokhzad, *Nat. Rev. Cancer*, 2017, **17**, 20–37.

9 U. Bulbake, S. Doppalapudi, N. Kommineni and W. Khan, *Pharmaceutics*, 2017, **9**(2), 12.

10 S. Wilhelm, A. J. Tavares, Q. Dai, S. Ohta, J. Audet, H. F. Dvorak and W. C. W. Chan, *Nat. Rev. Mater.*, 2016, **1**, 16014.

11 S. Yang and H. Gao, *Pharmacol. Res.*, 2017, **126**, 97–108.

12 S. C. Gupta, J. H. Kim, S. Prasad and B. B. Aggarwal, *Cancer Metastasis Rev.*, 2010, **29**, 405–434.

13 H. Gao, *Curr. Drug Metab.*, 2016, **17**, 731–736.

14 M. Overchuk and G. Zheng, *Biomaterials*, 2018, **156**, 217–237.

15 M. R. Junntila and F. J. de Sauvage, *Nature*, 2013, **501**, 346–354.

16 R. K. Jain, *Nat. Med.*, 2003, **9**, 685–693.

17 S. Azzi, J. K. Hebda and J. Gavard, *Front. Oncol.*, 2013, **3**, 211.

18 K. D. Barlow, A. M. Sanders, S. Soker, S. Ergun and L. J. Metheny-Barlow, *Cancer Microenviron.*, 2013, **6**, 1–17.

19 J. Fang, H. Nakamura and H. Maeda, *Adv. Drug Delivery Rev.*, 2011, **63**, 136–151.

20 K. C. Valkenburg, A. E. de Groot and K. J. Pienta, *Nat. Rev. Clin. Oncol.*, 2018, **15**, 366–381.

21 E. G. Neilson, N. A. Bhowmick and H. L. Moses, *Nature*, 2004, **432**, 332–337.

22 R. Kalluri, *Nat. Rev. Cancer*, 2016, **16**, 582–598.

23 X. Han, Y. Xu, M. Geranpayehvaghei, G. J. Anderson, Y. Li and G. Nie, *Biomaterials*, 2020, **232**, 119745.

24 O. Lieleg, R. M. Baumgartel and A. R. Bausch, *Biophys. J.*, 2009, **97**, 1569–1577.

25 T. Stylianopoulos, M. Poh, N. Insin, M. G. Bawendi, D. Fukumura, L. L. Munn and R. K. Jain, *Biophys. J.*, 2010, **99**, 1342–1349.

26 G. Qiu, M. Jin, J. Dai, W. Sun, J. Feng and W. Jin, *Trends Pharmacol. Sci.*, 2017, **38**, 669–686.

27 C. Roma-Rodrigues, R. Mendes, P. Baptista and A. Fernandes, *Int. J. Mol. Sci.*, 2019, **20**, 840.

28 L. Schito and G. L. Semenza, *Trends Cancer*, 2016, **2**, 758.

29 G. Jiménez-Valerio and O. Casanovas, *Trends Cancer*, 2017, **3**, 10–18.

30 C. Corbet and O. Feron, *Nat. Rev. Cancer*, 2017, **17**, 577–593.

31 S. Musetti and L. Huang, *ACS Nano*, 2018, **12**, 11740–11755.

32 H. Phuengkham, L. Ren, I. W. Shin and Y. T. Lim, *Adv. Mater.*, 2019, **31**, e1803322.

33 J. Nam, S. Son, K. S. Park, W. Zou, L. D. Shea and J. J. Moon, *Nat. Rev. Mater.*, 2019, **4**, 398–414.

34 B. Zhang, Y. Hu and Z. Pang, *Front. Pharmacol.*, 2017, **8**, 952.

35 D. H. Munn and V. Bronte, *Curr. Opin. Immunol.*, 2016, **39**, 1–6.

36 J. E. Talmadge and D. I. Gabrilovich, *Nat. Rev. Cancer*, 2013, **13**, 739–752.

37 I. Waldhauer and A. Steinle, *Oncogene*, 2008, **27**, 5932–5943.

38 M. Buoncervello, L. Gabriele and E. Toschi, *Int. J. Mol. Sci.*, 2019, **20**, 4320.

39 T. Ojha, V. Pathak, Y. Shi, W. E. Hennink, C. T. W. Moonen, G. Storm, F. Kiessling and T. Lammers, *Adv. Drug Delivery Rev.*, 2017, **119**, 44–60.

40 D. W. Siemann, *Cancer Treat. Rev.*, 2010, **37**, 63–74.

41 W. Song, Z. Tang, D. Zhang, H. Yu and X. Chen, *Small*, 2015, **11**, 3755–3761.

42 J. Jiang, N. Shen, T. Ci, Z. Tang, Z. Gu, G. Li and X. Chen, *Adv. Mater.*, 2019, **31**, 1904278.

43 Y. Liang, Y. Hao, Y. Wu, Z. Zhou, J. Li, X. Sun and Y. Liu, *ACS Appl. Mater. Interfaces*, 2019, **11**, 21381–21390.

44 N. Shen, J. Wu, C. Yang, H. Yu, S. Yang, T. Li, J. Chen, Z. Tang and X. Chen, *Nano Lett.*, 2019, **19**, 8021–8031.

45 S. Yang, Z. Tang, C. Hu, D. Zhang, N. Shen, H. Yu and X. Chen, *Adv. Mater.*, 2019, **31**, 1805955.

46 H. Qin, H. Yu, J. Sheng, D. Zhang, N. Shen, L. Liu, Z. Tang and X. Chen, *Adv. Sci.*, 2019, **6**, 1900327.

47 S. Kunjachan, A. Detappe, R. Kumar, T. Ireland, L. Cameron, D. E. Biancur, V. Motto-Ros, L. Sancey, S. Sridhar and G. M. Makrigiorgos, *et al.*, *Nano Lett.*, 2015, **15**, 7488–7496.

48 M. Guan, Y. Zhou, S. Liu, D. Chen, J. Ge, R. Deng, X. Li, T. Yu, H. Xu and D. Sun, *et al.*, *Biomaterials*, 2019, **213**, 119218.

49 W. Gao, S. Li, Z. Liu, Y. Sun, W. Cao, L. Tong, G. Cui and B. Tang, *Biomaterials*, 2017, **139**, 1–11.

50 V. P. Chauhan, T. Stylianopoulos, J. D. Martin, Z. Popović, O. Chen, W. S. Kamoun, M. G. Bawendi, D. Fukumura and R. K. Jain, *Nat. Nanotechnol.*, 2012, **7**, 383–388.

51 T. Stylianopoulos and R. K. Jain, *Proc. Natl. Acad. Sci. U. S. A.*, 2013, **110**, 18632–18637.

52 R. S. Heist, D. G. Duda, D. V. Sahani, M. Ancukiewicz, P. Fidias, L. V. Sequist, J. S. Temel, A. T. Shaw, N. A. Pennell and J. W. Neal, *et al.*, *Proc. Natl. Acad. Sci. U. S. A.*, 2015, **112**, 1547–1552.

53 Y. Sung, P. Jin, L. Chu, F. Hsu, M. Wang, C. Chang, S. Chiou, J. T. Qiu, D. Gao and C. Lin, *et al.*, *Nat. Nanotechnol.*, 2019, **14**, 1160–1169.

54 L. Tian, A. Goldstein, H. Wang, L. E. Dobrolecki, X. Zhang, N. Putluri, A. Sreekumar, M. A. M. William and X. H. F. Zhang, *Nature*, 2017, **544**, 250–254.

55 W. Yu, R. Liu, Y. Zhou and H. Gao, *ACS Cent. Sci.*, 2020, **6**, 100–116.

56 L. Schuster, O. Seifert, S. Vollmer, R. E. Kontermann, B. Schlosshauer and H. Hartmann, *Mol. Pharmaceutics*, 2015, **12**, 3146–3157.

57 G. Xiong, L. Deng, J. Zhu, P. G. Rychahou and R. Xu, *BMC Cancer*, 2014, **14**, 1.

58 X. Han, Y. Li, Y. Xu, X. Zhao, Y. Zhang, X. Yang, Y. Wang, R. Zhao, G. J. Anderson and Y. Zhao, *et al.*, *Nat. Commun.*, 2018, **9**, 3318–3390.

59 A. G. Kohli, S. Kivimäe, M. R. Tiffany and F. C. Szoka, *J. Controlled Release*, 2014, **191**, 105–114.

60 A. Kultti, S. Pasonen-Seppänen, M. Jauhainen, K. J. Rilla, R. Kärnä, E. Pyöriä, R. H. Tammi and M. I. Tammi, *Exp. Cell Res.*, 2009, **315**, 1914–1923.

61 V. Raeesi and W. C. W. Chan, *Nanoscale*, 2016, **8**, 12524–12530.

62 S. Lee, H. Han, H. Koo, J. H. Na, H. Y. Yoon, K. E. Lee, H. Lee, H. Kim, I. C. Kwon and K. Kim, *J. Controlled Release*, 2017, **263**, 68–78.

63 A. Zinger, L. Koren, O. Adir, M. Poley, M. Alyan, Z. Yaari, N. Noor, N. Krinsky, A. Simon and H. Gibori, *et al.*, *ACS Nano*, 2019, **13**, 11008–11021.

64 H. Gong, Y. Chao, J. Xiang, X. Han, G. Song, L. Feng, J. Liu, G. Yang, Q. Chen and Z. Liu, *Nano Lett.*, 2016, **16**, 2512–2521.

65 H. Zhou, Z. Fan, J. Deng, P. K. Lemons, D. C. Arhontoulis, W. B. Bowne and H. Cheng, *Nano Lett.*, 2016, **16**, 3268–3277.

66 B. Zhang, T. Jiang, S. Shen, X. She, Y. Tuo, Y. Hu, Z. Pang and X. Jiang, *Biomaterials*, 2016, **103**, 12–21.

67 X. Dong, H. Liu, H. Feng, S. Yang, X. Liu, X. Lai, Q. Lu, J. F. Lovell, H. Chen and C. Fang, *Nano Lett.*, 2019, **19**, 997–1008.

68 D. F. Mardhian, G. Storm, R. Bansal and J. Prakash, *J. Controlled Release*, 2018, **290**, 1–10.

69 L. Qin and H. Gao, *Asian J. Pharm. Sci.*, 2019, **14**, 380–390.

70 Z. Guo, K. Hu, J. Sun, T. Zhang, Q. Zhang, L. Song, X. Zhang and N. Gu, *ACS Appl. Mater. Interfaces*, 2014, **6**, 10963–10968.

71 X. Hu, P. He, G. Qi, Y. Gao, Y. Lin, C. Yang, P. Yang, H. Hao, L. Wang and H. Wang, *ACS Nano*, 2017, **11**, 4086–4096.

72 T. Ji, Y. Ding, Y. Zhao, J. Wang, H. Qin, X. Liu, J. Lang, R. Zhao, Y. Zhang and J. Shi, *et al.*, *Adv. Mater.*, 2015, **27**, 1865–1873.

73 M. J. Ernsting, B. Hoang, I. Lohse, E. Undzys, P. Cao, T. Do, B. Gill, M. Pintilie, D. Hedley and S. Li, *J. Controlled Release*, 2015, **206**, 122–130.

74 L. Miao, Q. Liu, C. M. Lin, C. Luo, Y. Wang, L. Liu, W. Yin, S. Hu, W. Y. Kim and L. Huang, *Cancer Res.*, 2017, **77**, 719–731.

75 G. Ishii, A. Ochiai and S. Neri, *Adv. Drug Delivery Rev.*, 2016, **99**, 186–196.

76 X. Chen and E. Song, *Nat. Rev. Drug Discovery*, 2019, **18**, 99–115.

77 Y. Zhao, J. Cao, A. Melamed, M. Worley, A. Gockley, D. Jones, H. T. Nia, Y. Zhang, T. Stylianopoulos and A. S. Kumar, *et al.*, *Proc. Natl. Acad. Sci. U. S. A.*, 2019, **116**, 2210–2219.

78 K. Hu, L. Miao, T. J. Goodwin, J. Li, Q. Liu and L. Huang, *ACS Nano*, 2017, **11**, 4916–4925.

79 Y. Wei, Y. Wang, D. Xia, S. Guo, F. Wang, X. Zhang and Y. Gan, *ACS Appl. Mater. Interfaces*, 2017, **9**, 25138–25151.

80 J. D. Martin, M. Panagi, C. Wang, T. T. Khan, M. R. Martin, C. Voutouri, K. Toh, P. Papageorgis, F. Mpekris and C. Polydorou, *et al.*, *ACS Nano*, 2019, **13**, 6396–6408.

81 J. Liu, Q. Chen, L. Feng and Z. Liu, *Nano Today*, 2018, **21**, 55–73.

82 G. Song, C. Liang, H. Gong, M. Li, X. Zheng, L. Cheng, K. Yang, X. Jiang and Z. Liu, *Adv. Mater.*, 2015, **27**, 6110–6117.

83 W. L. Liu, T. Liu, M. Z. Zou, W. Y. Yu, C. X. Li, Z. Y. He, M. K. Zhang, M. D. Liu, Z. H. Li and J. Feng, *et al.*, *Adv. Mater.*, 2018, **30**, e1802006.

84 M. Gao, C. Liang, X. Song, Q. Chen, Q. Jin, C. Wang and Z. Liu, *Adv. Mater.*, 2017, **29**, 1701429.

85 W. Zhu, Z. Dong, T. Fu, J. Liu, Q. Chen, Y. Li, R. Zhu, L. Xu and Z. Liu, *Adv. Funct. Mater.*, 2016, **26**, 5490–5498.

86 L. H. Liu, Y. H. Zhang, W. X. Qiu, L. Zhang, F. Gao, B. Li, L. Xu, J. X. Fan, Z. H. Li and X. Z. Zhang, *Small*, 2017, **13**, 1701621.

87 P. Liu, X. Xie, X. Shi, Y. Peng, J. Ding and W. Zhou, *ACS Appl. Mater. Interfaces*, 2019, **11**, 48261–48270.

88 D. Zheng, B. Li, C. Li, J. Fan, Q. Lei, C. Li, Z. Xu and X. Zhang, *ACS Nano*, 2016, **10**, 8715–8722.

89 Y. Fan, T. Zhou, P. Cui, Y. He, X. Chang, L. Xing and H. Jiang, *Adv. Funct. Mater.*, 2019, **29**, 1806708.

90 X. Song, L. Feng, C. Liang, M. Gao, G. Song and Z. Liu, *Nano Res.*, 2017, **10**, 1200–1212.

91 Z. Yang, Q. Chen, J. Chen, Z. Dong, R. Zhang, J. Liu and Z. Liu, *Small*, 2018, **14**, e1803262.

92 W. Yu, T. Liu, M. Zhang, Z. Wang, J. Ye, C. X. Li, W. Liu, R. Li, J. Feng and X. Z. Zhang, *ACS Nano*, 2019, **13**, 1784–1794.

93 B. M. Bola, A. L. Chadwick, F. Michopoulos, K. G. Blount, B. A. Telfer, K. J. Williams, P. D. Smith, S. E. Critchlow and I. J. Stratford, *Mol. Cancer Ther.*, 2014, **13**, 2805–2816.

94 J. Li, K. Shi, Z. F. Sabet, W. Fu, H. Zhou, S. Xu, T. Liu, M. You, M. Cao and M. Xu, *et al.*, *Sci. Adv.*, 2019, **5**, x937.

95 M. Ovais, M. Guo and C. Chen, *Adv. Mater.*, 2019, **31**, 1808303.

96 S. Zanganeh, G. Hutter, R. Spitzer, O. Lenkov, M. Mahmoudi, A. Shaw, J. S. Pajarinen, H. Nejadnik, S. Goodman and M. Moseley, *et al.*, *Nat. Nanotechnol.*, 2016, **11**, 986–994.

97 V. Mulens-Arias, J. M. Rojas, S. Pérez-Yagüe, M. P. Morales and D. F. Barber, *Biomaterials*, 2015, **52**, 494–506.

98 H. Shime, M. Matsumoto, H. Oshiumi, S. Tanaka, A. Nakane, Y. Iwakura, H. Tahara, N. Inoue and T. Seya, *Proc. Natl. Acad. Sci. U. S. A.*, 2012, **109**, 2066–2071.

99 C. Xu, S. Yang, Z. Jiang, J. Zhou and J. Yao, *Nano Lett.*, 2020, **20**, 372–383.

100 D. Chen, J. Xie, R. Fiskesund, W. Dong, X. Liang, J. Lv, X. Jin, J. Liu, S. Mo and T. Zhang, *et al.*, *Nat. Commun.*, 2018, **9**, 873.

101 Z. Nemeth, E. Csizmadia, L. Vikstrom, M. Li, K. Bisht, A. Feizi, S. Otterbein, B. Zuckerbraun, D. B. Costa and P. P. Pandolfi, *et al.*, *Oncotarget*, 2016, **7**, 23919.

102 C. Xu, S. Yang, Z. Jiang, J. Zhou and J. Yao, *Nano Lett.*, 2019, **20**, 372–383.

103 K. Sato, N. Sato, B. Xu, Y. Nakamura, T. Nagaya, P. L. Choyke, Y. Hasegawa and H. Kobayashi, *Sci. Transl. Med.*, 2016, **8**, 110r–352r.

104 Q. Song, Y. Yin, L. Shang, T. Wu, D. Zhang, M. Kong, Y. Zhao, Y. He, S. Tan and Y. Guo, *et al.*, *Nano Lett.*, 2017, **17**, 6366–6375.

105 M. Saeed, J. Gao, Y. Shi, T. Lammers and H. Yu, *Theranostics*, 2019, **9**, 7981–8000.

106 H. Yu, H. Lee, A. Herrmann, R. Buettner and R. Jove, *Nat. Rev. Cancer*, 2014, **14**, 736–746.

107 M. Huo, Y. Zhao, A. B. Satterlee, Y. Wang, Y. Xu and L. Huang, *J. Controlled Release*, 2017, **245**, 81–94.

108 Y. Zhao, M. Huo, Z. Xu, Y. Wang and L. Huang, *Biomaterials*, 2015, **68**, 54–66.

109 L. Jeanbart, I. C. Kourtis, A. J. van der Vlies, M. A. Swartz and J. A. Hubbell, *Cancer Immunol. Immunother.*, 2015, **64**, 1033–1046.

110 M. S. Sasso, G. Lollo, M. Pitorre, S. Solito, L. Pinton, S. Valpione, G. Bastiat, S. Mandruzzato, V. Bronte and I. Marigo, *et al.*, *Biomaterials*, 2016, **96**, 47–62.

111 D. Liu, B. Chen, Y. Mo, Z. Wang, T. Qi, Q. Zhang and Y. Wang, *Nano Lett.*, 2019, **19**, 6964–6976.

112 X. Han, K. Cheng, Y. Xu, Y. Wang, H. Min, Y. Zhang, X. Zhao, R. Zhao, G. J. Anderson and L. Ren, *et al.*, *J. Am. Chem. Soc.*, 2020, **142**, 2490–2496.

113 H. Huang, C. Jiang, S. Shen, A. Liu, Y. Gan, Q. Tong, S. Chen, Z. Gao, J. Du and J. Cao, *et al.*, *Nano Lett.*, 2019, **19**, 5356–5365.

114 L. Miao, J. Li, Q. Liu, R. Feng, M. Das, C. M. Lin, T. J. Goodwin, O. Dorosheva, R. Liu and L. Huang, *ACS Nano*, 2017, **11**, 8690–8706.

115 C. Li, J. Wang, G. Wei, Y. Huang, H. Yu, Y. Gan, Y. Wang, L. Mei, H. Chen and H. Hu, *et al.*, *Acta Pharm. Sin. B*, 2019, **9**, 1145–1162.

116 Z. M. Qian, *Pharmacol. Rev.*, 2002, **54**, 561–587.

117 M. Merino, S. Zalba and M. J. Garrido, *J. Controlled Release*, 2018, **275**, 162–176.

118 H. Gao, *Acta Pharm. Sin. B*, 2016, **6**, 268–286.

119 F. Araste, K. Abnous, M. Hashemi, S. M. Taghdisi, M. Ramezani and M. Alibolandi, *J. Controlled Release*, 2018, **292**, 141–162.

120 J. H. Lee, J. A. Engler, J. F. Collawn and B. A. Moore, *Eur. J. Biochem.*, 2001, **268**, 2004–2012.

121 X. Wei, C. Zhan, X. Chen, J. Hou, C. Xie and W. Lu, *Mol. Pharmaceutics*, 2014, **11**, 3261–3268.

122 H. Zhang, T. Wu, W. Yu, S. Ruan, Q. He and H. Gao, *ACS Appl. Mater. Interfaces*, 2018, **10**, 9094–9103.

123 M. Yu, D. Su, Y. Yang, L. Qin, C. Hu, R. Liu, Y. Zhou, C. Yang, X. Yang and G. Wang, *et al.*, *ACS Appl. Mater. Interfaces*, 2018, **11**, 176–186.

124 E. K. Duperret, A. Trautz, D. Ammons, A. Perales-Puchalt, M. C. Wise, J. Yan, C. Reed and D. B. Weiner, *Clin. Cancer Res.*, 2018, **24**, 1190–1201.

125 M. H. Sherman, R. T. Yu, D. D. Engle, N. Ding, A. R. Atkins, H. Tiriac, E. A. Collisson, F. Connor, T. Van Dyke and S. Kozlov, *et al.*, *Cell*, 2014, **159**, 80–93.

126 R. Yang, J. Xu, L. Xu, X. Sun, Q. Chen, Y. Zhao, R. Peng and Z. Liu, *ACS Nano*, 2018, **12**, 5121–5129.

127 S. Ruan, L. Qin, W. Xiao, C. Hu, Y. Zhou, R. Wang, X. Sun, W. Yu, Q. He and H. Gao, *Adv. Funct. Mater.*, 2018, **28**, 1802227.

128 R. Li, Y. He, S. Zhang, J. Qin and J. Wang, *Acta Pharm. Sin. B*, 2018, **8**, 14–22.

129 Y. Lu, Q. Hu, C. Jiang and Z. Gu, *Curr. Opin. Biotechnol.*, 2019, **58**, 81–91.

130 M. Zhang, J. Ye, Y. Xia, Z. Wang, C. Li, X. Wang, W. Yu, W. Song, J. Feng and X. Zhang, *ACS Nano*, 2019, **13**, 14230–14240.

131 B. Nieswandt and S. P. Watson, *Blood*, 2003, **102**, 449–461.

132 M. Feng, J. Y. Chen, R. Weissman-Tsukamoto, J. Volkmer, P. Y. Ho, K. M. McKenna, S. Cheshier, M. Zhang, N. Guo and P. Gip, *et al.*, *Proc. Natl. Acad. Sci. U. S. A.*, 2015, **112**, 2145–2150.

133 R. Liu, Y. An, W. Jia, Y. Wang, Y. Wu, Y. Zhen, J. Cao and H. Gao, *J. Controlled Release*, 2020, **321**, 589–601.

134 J. Xue, Z. Zhao, L. Zhang, L. Xue, S. Shen, Y. Wen, Z. Wei, L. Wang, L. Kong and H. Sun, *et al.*, *Nat. Nanotechnol.*, 2017, **12**, 692–700.

135 E. Kolaczewska and P. Kubes, *Nat. Rev. Immunol.*, 2013, **13**, 159–175.

136 Y. Huang, X. Gao and J. Chen, *Acta Pharm. Sin. B*, 2018, **8**, 4–13.

137 L. Guo, Y. Zhang, Z. Yang, H. Peng, R. Wei, C. Wang and M. Feng, *ACS Nano*, 2019, **13**, 1078.

138 D. Ha, N. Yang and V. Nadithe, *Acta Pharm. Sin. B*, 2016, **6**, 287–296.

139 J. Wang, Y. Dong, Y. Li, W. Li, K. Cheng, Y. Qian, G. Xu, X. Zhang, L. Hu and P. Chen, *et al.*, *Adv. Funct. Mater.*, 2018, **28**, 1707360.

140 W. Fu, C. Lei, S. Liu, Y. Cui, C. Wang, K. Qian, T. Li, Y. Shen, X. Fan and F. Lin, *et al.*, *Nat. Commun.*, 2019, **10**, 4355.

141 M. Li, S. Li, H. Zhou, X. Tang, Y. Wu, W. Jiang, Z. Tian, X. Zhou, X. Yang and Y. Wang, *Nat. Commun.*, 2020, **11**, 1126.

142 J. Z. Du, H. J. Li and J. Wang, *Acc. Chem. Res.*, 2018, **51**, 2848–2856.

143 Y. R. Zhang, R. Lin, H. J. Li, W. L. He, J. Z. Du and J. Wang, *Wiley Interdiscip. Rev.: Nanomed. Nanobiotechnol.*, 2019, **11**, e1519.

144 B. Chen, W. Dai, B. He, H. Zhang, X. Wang, Y. Wang and Q. Zhang, *Theranostics*, 2017, **7**, 538–558.

145 W. Gao, Y. Hu, L. Xu, M. Liu, H. Wu and B. He, *Chin. Chem. Lett.*, 2018, **29**, 1795–1798.

146 C. Chen, Y. Li, X. Yu, Q. Jiang, X. Xu, Q. Yang and Z. Qian, *Chin. Chem. Lett.*, 2018, **29**, 1609–1612.

147 J. Ding, J. Chen, L. Gao, Z. Jiang, Y. Zhang, M. Li, Q. Xiao, S. S. Lee and X. Chen, *Nano Today*, 2019, **29**, 100800.

148 X. Feng, H. Dixon, H. Glen Ravenhill, S. Karaosmanoglu, Q. Li, L. Yan and X. Chen, *Adv. Ther.*, 2019, **2**, 1900093.

149 W. Yu, M. Shevtsov, X. Chen and H. Gao, *Chin. Chem. Lett.*, 2020, DOI: 10.1016/j.cclet.2020.02.036.

150 Z. Zhang, H. Wang, T. Tan, J. Li, Z. Wang and Y. Li, *Adv. Funct. Mater.*, 2018, **28**, 1801840.

151 C. Hu, X. Cun, S. Ruan, R. Liu, W. Xiao, X. Yang, Y. Yang, C. Yang and H. Gao, *Biomaterials*, 2018, **168**, 64–75.

152 J. Chen, J. Ding, Y. Wang, J. Cheng, S. Ji, X. Zhuang and X. Chen, *Adv. Mater.*, 2017, **29**.

153 R. Kumari, D. Sunil and R. S. Ningthoujam, *J. Controlled Release*, 2020, **319**, 135–156.

154 Y. Niu, J. Zhu, Y. Li, H. Shi, Y. Gong, R. Li, Q. Huo, T. Ma and Y. Liu, *J. Controlled Release*, 2018, **277**, 35–47.

155 X. Zhang, L. An, Q. Tian, J. Lin and S. Yang, *J. Mater. Chem. B*, 2020, DOI: 10.1039/d0tb00030b.

156 Y. Li, X. Xu, X. Zhang, Y. Li, Z. Zhang and Z. Gu, *ACS Nano*, 2017, **11**, 416–429.

157 Q. Lei, S. Wang, J. Hu, Y. Lin, C. Zhu, L. Rong and X. Zhang, *ACS Nano*, 2017, **11**, 7201–7214.

158 S. Ruan, X. Cao, X. Cun, G. Hu, Y. Zhou, Y. Zhang, L. Lu, Q. He and H. Gao, *Biomaterials*, 2015, **60**, 100–110.

159 Y. L. Su, T. W. Yu, W. H. Chiang, H. C. Chiu, C. H. Chang, C. S. Chiang and S. H. Hu, *Adv. Funct. Mater.*, 2017, **27**, 1700056.

160 R. Liu, C. Hu, Y. Yang, J. Zhang and H. Gao, *Acta Pharm. Sin. B*, 2019, **9**, 410–420.

161 C. Song, Y. Li, T. Li, Y. Yang, Z. Huang, J. M. de la Fuente, J. Ni and D. Cui, *Adv. Funct. Mater.*, 2020, 1906309.

162 R. Liu, W. Xiao, C. Hu, R. Xie and H. Gao, *J. Controlled Release*, 2018, **28**, 127–139.

163 W. Xiao, S. Ruan, W. Yu, R. Wang, C. Hu, R. Liu and H. Gao, *Mol. Pharmaceutics*, 2017, **14**, 3489–3498.

164 Y. Cong, L. Ji, Y. J. Gao, F. H. Liu, D. B. Cheng, Z. Hu, Z. Y. Qiao and H. Wang, *Angew. Chem., Int. Ed.*, 2019, **58**, 4632–4637.

165 Y. Li, H. Y. Yang, T. Thambi, J. Park and D. S. Lee, *Biomaterials*, 2019, **217**, 119299.

166 X. Chen, L. Liu and C. Jiang, *Acta Pharm. Sin. B*, 2016, **6**, 261–267.

167 M. Kanamala, W. R. Wilson, M. Yang, B. D. Palmer and Z. Wu, *Biomaterials*, 2016, **85**, 152–167.

168 J. Cao, X. Xie, A. Lu, B. He, Y. Chen, Z. Gu and X. Luo, *Biomaterials*, 2014, **35**, 4517–4524.

169 H. Han, D. Valdeperez, Q. Jin, B. Yang, Z. Li, Y. Wu, B. Pelaz, W. J. Parak and J. Ji, *ACS Nano*, 2017, **11**, 1281–1291.

170 S. Li, W. Wu, K. Xiu, F. Xu, Z. Li and J. Li, *J. Biomed. Nanotechnol.*, 2014, **10**, 1480–1489.

171 T. Thambi, V. G. Deepagan, H. Y. Yoon, H. S. Han, S. Kim, S. Son, D. Jo, C. Ahn, Y. D. Suh and K. Kim, *et al.*, *Biomaterials*, 2014, **35**, 1735–1743.

172 S. Son, N. V. Rao, H. Ko, S. Shin, J. Jeon, H. S. Han, V. Q. Nguyen, T. Thambi, Y. D. Suh and J. H. Park, *Int. J. Biol. Macromol.*, 2018, **110**, 399–405.

173 J. Yan, H. Zhang, F. Cheng, Y. He, T. Su, X. Zhang, M. Zhang, Y. Zhu, C. Li and J. Cao, *et al.*, *Int. J. Nanomed.*, 2018, **13**, 8247–8268.

174 Z. Dong, L. Feng, W. Zhu, X. Sun, M. Gao, H. Zhao, Y. Chao and Z. Liu, *Biomaterials*, 2016, **110**, 60–70.

175 K. H. Min, H. S. Min, H. J. Lee, D. J. Park, J. Y. Yhee, K. Kim, I. C. Kwon, S. Y. Jeong, O. F. Silvestre and X. Chen, *et al.*, *ACS Nano*, 2015, **9**, 134–145.

176 Q. Sun, Z. Zhou, N. Qiu and Y. Shen, *Adv. Mater.*, 2017, **29**, 1606628.

177 H. C. Dietz, *J. Clin. Invest.*, 2010, **120**, 403–406.

178 X. Cun, S. Ruan, J. Chen, L. Zhang, J. Li, Q. He and H. Gao, *Acta Biomater.*, 2016, **31**, 186–196.

179 W. Xiao and H. Gao, *Int. J. Pharm.*, 2018, **552**, 328–339.

180 A. Salvati, A. S. Pitek, M. P. Monopoli, K. Prapainop, F. B. Bombelli, D. R. Hristov, P. M. Kelly, C. Åberg, E. Mahon and K. A. Dawson, *Nat. Nanotechnol.*, 2013, **8**, 137–143.

181 W. Xiao, J. Xiong, S. Zhang, Y. Xiong, H. Zhang and H. Gao, *Int. J. Pharm.*, 2018, **538**, 105–111.

182 A. Kolate, D. Baradaria, S. Patil, I. Vhora, G. Kore and A. Misra, *J. Controlled Release*, 2014, **192**, 67–81.

183 Y. Fang, J. Xue, S. Gao, A. Lu, D. Yang, H. Jiang, Y. He and K. Shi, *Drug Delivery*, 2017, **24**, 22–32.

184 V. Juang, C. H. Chang, C. S. Wang, H. E. Wang and Y. L. Lo, *Small*, 2019, **15**, 1903296.

185 R. Cheng, F. Feng, F. Meng, C. Deng, J. Feijen and Z. Zhong, *J. Controlled Release*, 2011, **152**, 2–12.

186 Z. Fang, S. Pan, P. Gao, H. Sheng, L. Li, L. Shi, Y. Zhang and X. Cai, *Int. J. Pharm.*, 2019, **575**, 118841.

187 S. Ruan, X. Cao, X. Cun, G. Hu, Y. Zhou, Y. Zhang, L. Lu, Q. He and H. Gao, *Biomaterials*, 2015, **60**, 100–110.